

CERTIFICATE OF MAILING BY "FIRST CLASS MAIL"

I hereby certify that this correspondence is being deposited with the United States Postal Service as first class mail in an envelope addressed to:
Assistant Commissioner for Patents, Washington, D.C. 20231, on June 4, 2001.

Jami M. Procopio



IN THE UNITED STATES PATENT AND TRADEMARK OFFICE

In the application of:

Terry P. Snutch, *et al.*

Serial No.: 09/030,482

Filing Date: 25 February 1998

For: NOVEL HUMAN CALCIUM
CHANNELS AND RELATED PROBES,
CELL LINES AND METHODS

Examiner: Nirmal S. Basi

Group Art Unit: 1646

EXPEDITED PROCEDURE --
EXAMINING GROUP 1646

DECLARATION OF DR. TERRANCE SNUTCH

Assistant Commissioner for Patents
Washington, D.C. 20231

Dear Sir:

I, Terrance Snutch, declare as follows:

1. I am a co-inventor of the subject matter claimed in the above-referenced application and have been practicing in the field of molecular biology, and specifically in the field of ion channels, for over 15 years. A copy of my *curriculum vitae* is attached hereto as Exhibit A. I have published many papers on the structure and function of calcium channels and am considered one of the leading researchers in this field.

2. The nucleotide sequence set forth as SEQ. ID. NO: 18 encodes about 85% of the total amino acid sequence, starting at the exact N-terminus, of a member of a family of voltage-gated ion channels that contain four homologous structural domains (domains I, II, III and IV). All of the identified members of this four-domain class of ion channels are either voltage-gated

Exhibit A

calcium or sodium ion channels. In each case, each of the four homologous domains contains structural elements necessary for channel function. Each contains six transmembrane segments including a transmembrane segment called the S4 region that acts as the voltage sensor of the channel. Also contained in each homologous domain is a region called the P-loop or Pore region that contains specific amino acid residues responsible for ion selectivity. Voltage-gated sodium and calcium channels can easily be distinguished from each other based upon their overall degree of sequence conservation and by the specific amino acid residues that constitute the Pore region responsible for ion flux (see below).

3. I have concluded that SEQ. ID. NO: 18 encodes virtually the entire amino acid sequence of a major branch of the calcium channel family that represents a T-type channel. The calcium channel family and the evolutionary relationships between its members are shown in Figure 1. The construction of the family is based on sequence homology in the genes encoding the various members. As seen in Figure 1, a closely related branch of the family is represented by several types designated P/Q, N and R; this major branch is more distantly related to another branch which is represented by various L-type channels. The nucleotide sequence set forth in the present invention as SEQ. ID. NO: 18 has characteristics which place it in this general family, but it is relatively distantly related to the two branches represented by the α_1 subunits A, B, E and α_1 subunits S, C and D. My conclusion that Figure 1 represents an accurate characterization of SEQ. ID. NO: 18 is based on the reasoning set forth in paragraphs 4-6 below.

4. Over the past 30 years native calcium channels have been classified into high-threshold (L-type, N-type, P/Q-type and R-type) or low threshold subtypes (T-type), as illustrated in Figure 1. The placement of the high-voltage types is based on evolutionary analysis of already cloned calcium channels. This shows that the P/Q-type, N-type and R-type calcium channel α_1 subunits constitute one branch of calcium channels while the L-type subunits α_1C , α_1D and α_1S constitute a second evolutionary branch. The only class of calcium channel not accounted for is the third branch which would thus include the T-type. Comparison of SEQ. ID. NO: 18 deduced amino acid with that of the other α_1 subunits clearly indicates that it forms a third evolutionary class of calcium channel, which based upon physiological and pharmacological criteria must represent the T-type channel.

5. Examination of the Pore region of SEQ. ID. NO: 18 compared to the high threshold calcium channels and also sodium channels indicates that SEQ. ID. NO: 18 encodes a novel type

of calcium channel. In all high threshold calcium channels, the pore region of each domain (I, II, III, and IV) contains a glutamate residue (E) that is responsible for the selective flux of calcium through the channel (Yang, *et al.*, 1993, "Molecular Determinants of Ca Selectivity and Ion Permeation in L-type Ca Channels," *Nature* 366:158-161). In contrast, sodium channels possess other amino acids in the analogous positions (domain I = aspartate (D), domain II = glutamate (E), domain III = lysine (K). Mutation of the domain III lysine (K) of sodium channels to the corresponding glutamate (E) found in the high threshold calcium channels results in the flux of calcium and indicates that the domain III pore region is critical to defining ion flux (Heinemann, *et al.*, 1992, "Calcium Channel Characteristics Conferred on the Sodium Channel by Single Mutations," *Nature* 356:441-443). It is known from the behavior of the calcium channels whose genes had not yet been cloned that these "T-type" calcium channels possess distinct permeation properties compared to high-threshold calcium channels. In general, while high-threshold calcium channels flux barium at a higher rate than calcium, T-type channels flux calcium at a similar or higher rate than that for barium (for review, see Huguenard, 1996, "Low-Threshold Calcium Currents in the Central Nervous System Neurons" *Annu. Rev. Physiol.* 58:329-348). Examination of the Pore region of SEQ. ID. NO: 18 shows that in domain III it contains the substitution of an aspartate residue (D) for the glutamate residue (E) that is absolutely conserved in all of the high threshold calcium channels. A comparison of the relevant positions in the Pore regions of domains I, II and III of the known calcium channels, the sodium channel, and SEQ. ID. NO: 18 is shown in Figure 2. Since the domain III glutamate (E) residue of the high threshold calcium channels is critical for ion flux (Yang, *et al.*, 1993, *supra*), one can conclude that the substitution of D for E in SEQ. ID. NO: 18 contributes to the unique permeation properties of the T-type channel.

6. The intracellular linker region separating domains I and II of all high threshold calcium channels contains a high-affinity binding site for the calcium channel β subunit. The consensus β subunit binding site found in the N-type, P/Q-type, L-type and R-type channels is: QQ-E—L-GY—WI---E and is a defining characteristic of high threshold calcium channels (Pragnell, *et al.*, 1994 "Calcium Channel β -Subunit Binds to a Conserved Motif in the I-II Cytoplasmic Linker of the α_1 Subunit," *Nature* 368:67-70). It is known that T-type calcium channels do not contain or bind to the β subunit of high threshold calcium channels. The amino

acid sequence encoded by SEQ. ID. NO: 18 does not possess the consensus β subunit binding sequence. This is consistent with SEQ. ID. NO: 18 encoding a T-type calcium channel.

7. For the reasons set forth in paragraphs 4-6, I am certain that SEQ. ID. NO: 18 encodes a T-type calcium ion channel α_1 subunit. To summarize, as set forth in paragraph 4, a comparison of the deduced amino acid sequence in SEQ. ID. NO: 18 with that of other known four-domain voltage gated channels shows that it is relatively distantly related from the calcium channels whose genes have already been cloned and amino acid sequences deduced and thus belongs to the low-threshold subtype (T-type) which had not heretofore been cloned; paragraph 5 demonstrates that the critical amino acids in the Pore region verify that it is a calcium ion channel rather than a sodium ion channel and that it is distinct from the already cloned high-threshold channels, and paragraph 6 demonstrates that as expected, the deduced amino acid sequence lacks a β subunit binding sequence. The coding sequence is not entirely complete (approximately 85%), but it is sufficient both to (1) verify its nature as encoding a T-type calcium ion channel subunit and (2) to provide sufficient information to permit supplementation with additional nucleotide sequence to encode a functional T-type channel without retrieving a full length clone.

8. SEQ. ID. NO: 18 contains an ATG start codon that precedes three complete homologous structural domains I, II and III, and up to the S1 transmembrane segment of domain IV. Each of the domains I through III possesses an intact voltage sensor segment (S4) as well as a complete Pore region. Since structural domains II, III and IV result from the evolutionary duplication of domain I, SEQ. ID. NO: 18 contains sufficient information to construct a complete domain IV and thus a functional T-type calcium channel α_1 subunit. The nature of the amino acid sequence in domain IV can be surmised from the amino acid sequence of domain III. Of course, means to construct a nucleotide sequence extending the nucleotide sequence of SEQ. ID. NO: 18 to include a nucleotide sequence encoding this deduced amino acid sequence are routine.

9. In summary, one of ordinary skill in the art given the information set forth in SEQ. ID. NO: 18

(a) would understand that it encodes about 85% of a functional T-type calcium channel α_1 subunit starting at the N-terminus,

(b) would be able to design an amino acid sequence representing the missing C-terminal portion based on homology to the three domains encoded by SEQ. ID. NO: 18, and

(c) would be able to construct an expression system containing a nucleotide sequence encoding a functional T-type calcium ion channel α_1 subunit without obtaining a full length clone.

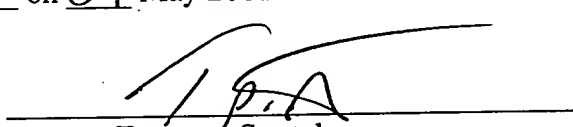
10. In addition to the foregoing demonstration that the application discloses the essential features of a T-type calcium channel, I further provide information regarding the nexus between all T-type calcium channels and identified conditions which can be treated with compounds that interact with T-type calcium channels. There are several T-type calcium channels found in a single individual which vary slightly in structure and demonstrably in terms of their distribution among various tissues. The particular T-type calcium channel involved in a particular condition may depend on its tissue distribution; for instance, T-type channels found in the neuronal system are associated with epilepsy and neurological diseases in general where spastic convulsions are involved. However, it is not necessary to understand which particular T-type calcium channel is being used in a screen for compounds that would be useful in treating, for example, these convulsive conditions because of the similarity in the binding specificity of all T-type channels. In very simple terms, compounds which are found to inhibit the activity of neuronal T-type channels will also inhibit the activity of T-type channels found in other tissues. Thus, any arbitrarily chosen T-type channel could be expressed in a cell line for use in screening assays to identify antagonists and the antagonists would be useful in treating the conditions associated with any T-type channel. As noted in the accompanying response, abnormal T-type activity is associated with a number of cardiac conditions, with hypertension, with neurological diseases involving spastic convulsions, and with impaired fertility. An antagonist identified with regard to any T-type channel would be useful in all of these conditions.

11. The pattern of similar binding activity among all T-type channels can be analogized to such a pattern among L-type channels. All of the T-type channels have similar behaviors in that they activate at low membrane potential, have small single channel conductance, have negative steady state inactivation properties, and contribute to spike firing patterns and rhythmic bursting processes. Analogous to the T-type channel another type of channel linked by similar behaviors is the L-type. There are several α_1 subunits associated with various L-type channels - *i.e.*, α_{1S} , α_{1C} , and α_{1D} and each is encoded by a distinct gene and exhibits a distinct distribution

pattern. For example, α_{1S} is in skeletal muscle; α_{1C} is in neurons and cardiac and smooth muscle; and α_{1D} is found in neurons and endocrine cells. They can be discriminated from all other types of calcium channels by their common sensitivity to 1,4-dihydropyridines. Thus, any one of these genes could be used to generate an L-type calcium channel for use in a cell-based assay to identify antagonists. These identified antagonists would bind to all of these L-type channels and thus would be useful in treating conditions related to any one of them.

I declare that all statements made herein of my own knowledge are true and that all statements made on information and belief are believed to be true; and further, that these statements are made with the knowledge that willful, false statements and the like so made are punishable by fine or imprisonment or both, under Section 1001 of Title 18 of the United States Code and that such willful false statements may jeopardize the validity of the application or any patent issued thereon.

Executed at VANCOUVER, BC on 29 May 2001.


Terrance Snutch

PATENT
Docket No. 381092000700

CERTIFICATE OF MAILING BY "FIRST CLASS MAIL"

I hereby certify that this correspondence is being deposited with the United States Postal Service as first class mail in an envelope addressed to:
Assistant Commissioner for Patents, Washington, D.C. 20231, on October 10, 1998.

Keren LePari
Keren LePari

IN THE UNITED STATES PATENT AND TRADEMARK OFFICE

In the application of:

Terry P. Snutch, *et al.*

Serial No.: 09/030,482

Filing Date: 25 February 1998

For: NOVEL HUMAN CALCIUM
CHANNELS AND RELATED PROBES,
CELL LINES AND METHODS

Examiner: Nirmal S. Başı

Group Art Unit: 1646

DECLARATION OF TERRANCE P. SNUTCH

Assistant Commissioner for Patents
Washington, D.C. 20231

Dear Sir:

I, Terrance P. Snutch, declare as follows:

1. I am a co-inventor of the subject matter claimed in the above-referenced application and have been practicing in the field of molecular biology for over twenty years. I am very familiar with cloning techniques and hybridization conditions.

2. In my opinion, the designation of hybridization conditions as those of medium stringency would convey to those of skill in the art that nucleotide sequences encoding closely related members of the same family of molecules would hybridize, but those outside this closely related family would not. In the present case, it would be understood that members of the family

represented by the newly discovered ion channel family described herein would hybridize to the disclosed nucleotide sequences, but nucleotide sequences encoding ion channels presently known in the art would not.

3. There are many examples in the literature whereby hybridization stringency is referred to as high, medium or low based upon temperature and salt conditions (*e.g.* Snutch, T.P., Heschl, M.F.P. and Baillie, D.L. (1988). The *Caenorhabditis elegans* hsp70 gene family: a molecular genetic characterization. *Gene* 64:241-255; Yu, A.S.L., Hebert, S.C., Brenner, B.M. and Lytton, J. (1992). Molecular characterization and nephron distribution of a family of transcripts encoding the pore-forming subunit of Ca^{2+} channels in the kidney. *Proc. Natl. Acad. Sci. USA* 89:10494-10498).

4. Medium stringency hybridization to colony or plaque lifts fixed on nitrocellulose or nylon membranes is typically performed 62°C to 65°C in the presence of probe in a solution containing 5 times Denhardt's, 0.3% SDS and 5 X SSPE. Non-specific carrier DNA such as denatured salmon sperm DNA (100 to 200 ug/ml) and a hybridization accelerator such as dextran sulfate (10%) may also be included in the hybridization buffer. Alternatively, medium stringency hybridization may be performed at 42°C in a solution containing 50% formamide, 5 times Denhardt's, 0.3% SDS and 5 X SSPE. The exact concentration of SDS and SSPE can vary and there are reports of SDS utilized from 0.2% to 0.7% and SSPE from 5 X to 6 X or the alternative buffer SSC from 5 X to 6 X. After hybridization the hybridization solution is removed and membranes are washed several times in a solution typically containing 0.1 % to 0.3% SDS and 2 X SSPE to 0.2 X SSPE. The temperature of medium stringency washing typically can vary from 55°C to 65°C.

5. Detailed information concerning the relevant considerations to be taken into account for determining hybridization stringency can be found in: Basic Methods in Molecular Biology (1986) Edited by Davis, L.G., Dibner, M.D. and Battery, J.F. Elsevier Science

Publishing Co., New York, and in DNA Probes (1989) Edited by Keller, G.H and Manak, M.M. Stockton Press, New York.

I further declare that all statements made herein of my own knowledge are true and that all statements made on information and belief are believed to be true; and that these statements were made with the knowledge that willful false statements and the like so made are punishable by fine or imprisonment, or both, under Section 1001 of Title 18 of the United States Code, and that such willful false statements may jeopardize the validity of the application or any patent issuing thereon.

Executed at Vancouver, BC on 10 October 2000.



Terrance P. Snutch

REVIEW

Molecular Pharmacology of T-type Ca^{2+} Channels

Tiffany N. Heady¹, Juan C. Gomora², Timothy L. Macdonald¹ and Edward Perez-Reyes^{2,*}

¹Department of Chemistry, University of Virginia, Charlottesville, Virginia 22904, USA

²Department of Pharmacology, University of Virginia, Charlottesville, Virginia 22908, USA

Received November 9, 2000

ABSTRACT—Over the past few years increasing attention has been focused on T-type calcium channels and their possible physiological and pathophysiological roles. Efforts toward elucidating the exact role(s) of these calcium channels have been hampered by the lack of T-type specific antagonists, resulting in the subsequent use of less selective calcium channel antagonists. In addition, the activity of these blockers often varies with cell or tissue type, as well as recording conditions. This review summarizes a variety of compounds that exhibit varying degrees of blocking activity towards T-type Ca^{2+} channels. It is designed as an aid for researchers in need of antagonists to study the biophysical and pathological nature of T-type channels, as well as a starting point for those attempting to develop potent and selective antagonists of the channel.

Keywords: T-type calcium channel, Antihypertensive, Mibefradil, Antiepileptic, Anesthetic, Antipsychotic, Amiloride

Introduction

Calcium is essential for life and is the most common signal transduction element in cells. A staggering electrochemical gradient exists between its extracellular concentration of approximately 2 mM compared to resting intracellular concentrations of approximately 100 nM. Stimulation of cells can lead to increases in intracellular concentrations into the micromolar range, with much higher concentrations in microdomains. This calcium enters the cytosol either through plasma membrane ion channels or is released from intracellular pools. Plasma membrane ion channels can be classified as either receptor- or store-operated channels, which are usually non-selective for cations such as Na^+ and Ca^{2+} , or voltage-gated channels, which are highly selective for Ca^{2+} .

The diversity of voltage-gated calcium channels has been extensively studied using electrophysiological, biochemical, pharmacological, and more recently, using molecular biology techniques. Early voltage-clamp studies identified two main classes of channels: those that responded to small (10 mV) changes in the resting membrane potential, or low-voltage-activated (LVA), and those that required stronger (30 mV) depolarizations to open, or high-voltage-activated (HVA). Pharmacological studies allowed further dissection

of the HVA family into L-, N-, P-, Q-, and R-types (1). These studies relied heavily on toxins isolated from snails (*Conus*) and funnel-web spiders (*Agelenopsis*) (2). Cloning of ten $\alpha 1$ subunits of voltage-activated Ca^{2+} channels has allowed a new classification based on sequence similarities (3). Alignments reveal that there are three main subfamilies of $\alpha 1$ subunit: 1) $\text{Ca}_v 1$, which contains four members that encode L-type channels ($\text{Ca}_v 1.1$, $\alpha 1\text{S}$; $\text{Ca}_v 1.2$, $\alpha 1\text{C}$; $\text{Ca}_v 1.3$, $\alpha 1\text{D}$; and $\text{Ca}_v 1.4$, $\alpha 1\text{F}$, which has yet to be expressed); 2) $\text{Ca}_v 2$, which contains three members including the P- and Q-types (both encoded by $\text{Ca}_v 2.1$, $\alpha 1\text{A}$), the N-type ($\text{Ca}_v 2.2$, $\alpha 1\text{B}$), and R-type ($\text{Ca}_v 2.3$, $\alpha 1\text{E}$); and 3) $\text{Ca}_v 3$, which contains three members that encode T-type channels ($\text{Ca}_v 3.1$, $\alpha 1\text{G}$; $\text{Ca}_v 3.2$, $\alpha 1\text{H}$; and $\text{Ca}_v 3.3$, $\alpha 1\text{I}$). All of these $\alpha 1$ subunits contain structural motifs that have been extremely conserved during evolution. The most basic element appears to be a pore loop surrounded by two membrane spanning domains (4). During evolution, more membrane spanning regions were added, resulting in a structure containing 6 transmembrane regions and a pore loop. One of these transmembrane regions contains many positive charges, conferring voltage sensitivity to the channel. Such is the structure of many voltage-gated K^+ channels (K_v), which are composed of four of these subunits. The next step in evolution was to join four α subunits into a single molecule, which is the structure of both voltage-gated Ca^{2+} and Na^+ channels. This conservation of sequence and predicted

*Corresponding author: FAX: +1-804-982-3878
E-mail: eperez@virginia.edu

structure allows comparisons of these channels to the *Streptomyces* K⁺ channel whose structure was recently solved using X-ray crystallography (4). Such comparisons may be useful in understanding drug binding sites (5).

Biochemical studies established that HVA channels contain auxiliary subunits such as α_2 , β , δ , and γ . Subsequent studies showed that δ was encoded on the same gene as α_2 . Molecular cloning has revealed that each of these subunits contains other family members. There are now genes for three $\alpha_2\delta$ subunits, four β subunits and five γ subunits (6, 7). Coexpression studies of the cloned subunits indicates that auxiliary subunits can alter the pharmacological properties of the channel (8). Furthermore, auxiliary subunits themselves may be the target of drugs; for example, gabapentin binds with high affinity to $\alpha_2\delta$ (9). The structure of LVA channels has not been determined biochemically.

Although the subject of this review is the pharmacology of T-type calcium channels, it should be noted that presently there are no compounds that are highly selective for these channels. Studies on the pharmacology of T-type channels have been complicated by many factors. For one, these channels are rarely expressed alone, which means the currents can be contaminated by other ionic conductances, notably HVA channels. This leads to under-estimates of the drug's potency. Typically LVA currents are separated from HVA currents by changing the holding potential from -90 mV (where both are active) to -40 mV where only some HVA channels are active. However, the block of many ion channels is state-dependent, with up to 1000-fold higher affinity for partially inactivated states. This may also lead to under-estimates of a drug's selectivity because the effects are being measured on LVA channels in the resting state, while HVA channels may be partially inactivated. Most of the studies reported herein used resting membrane potentials ranging from -100 to -80 mV, so the reported IC₅₀ values are probably dominated by the affinity of the drug for the resting state. Second, T-type channels are typically expressed at low densities, so many studies have used high concentrations of charge carrier to amplify the small currents. Again, this may lead to under-estimates of potency because channel block is often reduced at high divalent cation concentrations. Although this effect is often attributed to interactions in the permeation pathway, it should be noted that surface charge screening may also play a role. Due to these considerations, the divalent cation and its concentration are noted in the tables.

Antihypertensives

Calcium channel blockers have been used since the early 1960s to treat a variety of cardiovascular diseases like hypertension, cardiac arrhythmia and angina pectoris (10). Traditional calcium channel antagonists fit into three distinct chemical classes, the phenylalkylamines (e.g., vera-

pamil), dihydropyridines (e.g., nifedipine) and benzothiazepines (e.g., diltiazem). Representative structures are shown in Fig. 1. In general, their beneficial effects are thought to be due to blocking smooth muscle L-type channels, leading to decreases in cytosolic Ca²⁺, and relaxation of vascular smooth muscle cells. An important property of these drugs is to block preferentially smooth muscle L-type channels with little effect on cardiac L-type channels. Many first generation calcium channel blockers blocked both, such as verapamil and diltiazem. Second generation blockers such as nimodipine display greater selectivity for vascular beds (11). Two mechanisms that contribute to this selectivity are: 1) state dependent block, where drugs preferentially block partially inactivated channels, and 2) tissue specific expression of Ca_v1.2 splice variants that have distinct sensitivity to the drugs (12).

Mibefradil (Ro 40-5967) was introduced to the market in 1997, but then abruptly withdrawn. It was approved for use in hypertension and angina and marketed as the first selective T-type Ca²⁺ channel blocker (13). Indeed, depending on the cell type, mibefradil blocks T-type Ca²⁺ channels 10 to 30 times more potently than L-type Ca²⁺ channels (14, 15). In addition, mibefradil is highly tissue selective, relaxing smooth muscle without inducing reflex tachycardia, or having much effect on cardiac chronotropy or inotropy (13, 16). However, pharmacokinetic interactions with other drugs metabolized by cytochromes P-450 3A4 and 2D6 (antihistamines, such as astemizole) eventually led to the withdrawal of mibefradil from the clinic.

Electrophysiological experiments in a wide variety of native T-type Ca²⁺ currents have shown mibefradil IC₅₀ values ranging from 0.1 to 4.7 μ M (Table 1). Vascular smooth muscle T-type currents have been the most sensitive to mibefradil with an IC₅₀ of 0.1–0.2 μ M (14). In contrast, T-type currents recorded from mouse spermatogenic cells were reported to be much less sensitive (IC₅₀ = 4.7 μ M (17)). Mibefradil blocks all three cloned T-type channels with similar potency (18), although Ca_v3.3 may be twofold less sensitive (19). Direct comparisons indicate that it blocks native and the cloned Ca_v3.2 channels with equal potency (20).

Mibefradil can also block HVA channels. In cultured spinal motoneurons, mibefradil blocked N, L-, and P/Q-type channels at similar concentrations (1.4 μ M) as the block of an LVA current (21). In cerebellar Purkinje neurons, mibefradil blocked P-type currents with an apparent IC₅₀ of 3 μ M; however, under identical conditions, it blocked T-type currents with an IC₅₀ of 14 nM (22). The major difference in these studies was the holding potential, which was -90 mV in the motoneuron study and -70 mV in the Purkinje neuron study. Although this discrepancy could be caused by differences in voltage-dependent block (discussed below), this does not appear to be the case (23).

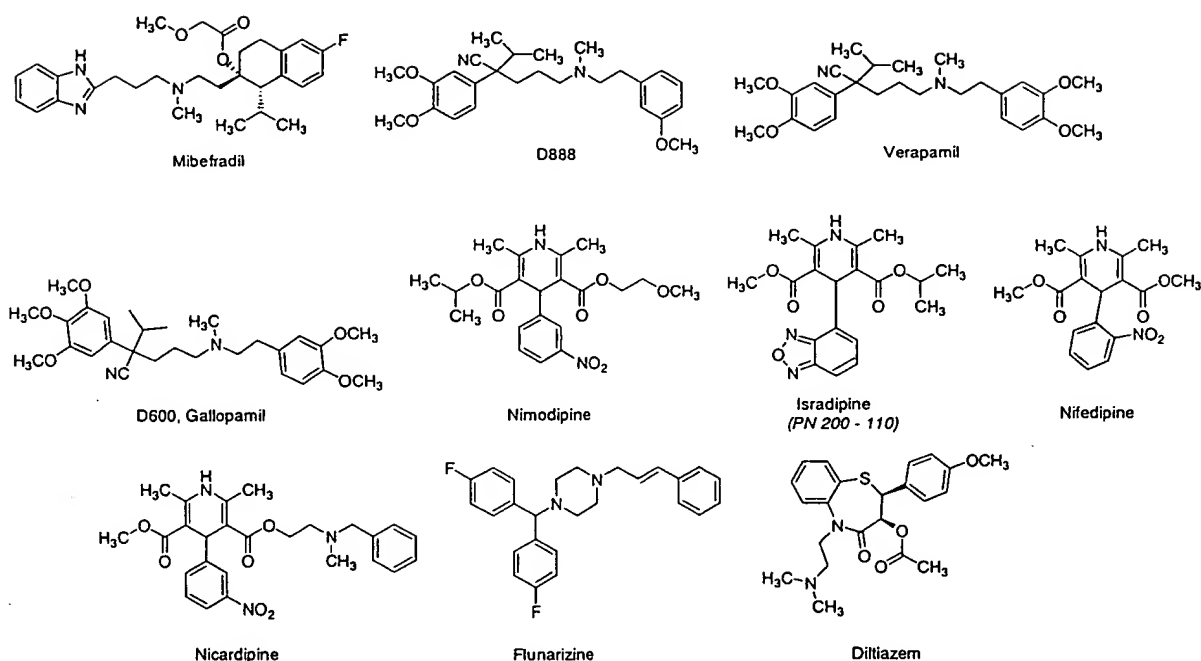


Fig. 1. Calcium channel blockers that also inhibit T-type channels.

Table 1. Calcium channel blockers that also inhibit T-type channels

| | Mibefradil | Verapamil | D600 | Amlodipine | Nimodipine | Isradipine | Nifedipine | Nicardipine | Flunarizine | Diltiazem | Reference |
|----------------------|-------------|-----------|------|------------|------------|------------|-----------------|-------------|-------------|-----------|--------------|
| Hypothalamus | | | 50 | | 7 | | 5 | 3.5 | 0.7 | 70 | (32) |
| Amygdala neurons | | | 65 | | | | | 2.5 | 1.1 | 120 | (84) |
| CA1 hippocampus | | | 120 | | | | | 1.6 | 1.2 | 210 | (85) |
| Cerebellar Purkinje | 1 | | | | | | | | | | (22) |
| Thalamus LD | | | | | | | 2.6 | | | | (33) |
| Retinal ganglion | | | | | | | 10 (50%) | | | | (86) |
| Motoneuron | 1.4 | | | | | | 10 (approx. 5%) | | | | (21) |
| Sensory neuron | 3 | | | | | 5 (11%) | 5 (19%) | 2 | | | (38, 50) |
| NG108-15 | 1 (50%) | | | | 10 (63%) | | | | | | (87) |
| NIE-115 | | | | | | | 30 (NE) | | 30 (40%) | | (88) |
| Atrial myocytes | 1.2 | | | 5.7 | | | | | | | (20) |
| Ventricular myocytes | | | | | | | | | 10 (80%) | | (89) |
| Aorta SMC | | 30 | | | | | | 0.6 | 0.1 | 30 | (39) |
| Azygos vein SMC | approx. 0.1 | | | | | | | | | | (14) |
| Adrenal fasciculata | 1.0 | | | | | | | | | | (27) |
| Spermatocytes | 5 | 70 | | | | 0.04 | 0.4 | | | | (61) |
| Pituitary GH3 | | | 51 | | | | 50 | | | 131 | (90) |
| Thyroid hMTC | 2.7 | 10 | | | | 4.7 | 10 (NE) | | | | (29) |
| Skeletal muscle | 0.7 | | | | | | | | | | (25) |
| Ca _v 3.1 | 0.4 – 1.2 | | | | | | | | | | (18, 19, 30) |
| Ca _v 3.2 | 1.1 – 1.2 | 1 (17%) | | 31 | 10 (44%) | | | | | | (18, 20, 67) |
| Ca _v 3.3 | 1.5 – 2.3 | | | | | | | | | | (18, 19) |

All concentrations reported are micromolar and represent the IC_{50} values determined from dose-response measurements. Studies where only a single concentration was studied are noted by giving the concentration and the percent inhibition observed or NE if no significant effect was observed. The charge carrier used in each study is as follows (in mM): (reference 32) 5 Ca^{2+} , (84) 10 Ca^{2+} , (85) 10 Ca^{2+} , (22) 5 Ba^{2+} , (33) 2 Ca^{2+} , (86) 10 Ca^{2+} , (21) 5 Ba^{2+} , (38) 5 Ba^{2+} , (50) 10 Ba^{2+} , (87) 10 Ba^{2+} , (88) 20 Ba^{2+} , (20) 1.8 Ca^{2+} , (89) 5.4 Ca^{2+} , (39) 20 Ca^{2+} , (14) 20 Ba^{2+} , (27) 10 Ca^{2+} , (61) 10 Ca^{2+} , (90) 10 Ca^{2+} , (29) 30 Ba^{2+} , (25) 10 Ba^{2+} , (18) 10 Ba^{2+} , (19) 2 Ca^{2+} , (30) 20 Ba^{2+} , (67) 15 Ba^{2+} .

Many studies indicate that mibefradil is also capable of blocking various other ion channels at micromolar concentrations. It can also block Ca^{2+} - and volume activated Cl^- channels of calf endothelial cells with IC_{50} s of approximately $5 \mu\text{M}$, while in the same preparation, the inwardly rectifying K^+ channel was not affected at concentrations up to $30 \mu\text{M}$ (24). In skeletal myoblasts, mibefradil blocked three voltage-gated K^+ currents, including an inward rectifier, a delayed rectifier, and a human *ether-a-go-go* with a respective IC_{50} of 5.6, 0.3 and $0.7 \mu\text{M}$ (25). The observation that mibefradil also blocks outward K^+ currents with similar potency as T-type currents was corroborated in adrenal zona fasciculata cells, where the ATP-activated K^+ current expressed was inhibited by mibefradil with an IC_{50} of $0.5 \mu\text{M}$ (26), a concentration twofold lower than that required to inhibit T-type Ca^{2+} currents under similar conditions (27). The effect of mibefradil on K^+ currents suggest that, in the case of cardiac cells, the action potential duration, resting membrane potential or even rhythmic activity could be altered by this drug. As a result, ventricular arrhythmias may occur, and this could explain in part the cardiovascular toxicity of this drug when used in combination with antihistamines. Finally, binding experiments showed that nanomolar concentrations of mibefradil can compete with [^3H]-WIN17317-3 binding to Na^+ channels of guinea pig synaptic membranes; this observation was confirmed with electrophysiological experiments using GH3 cells, whose Na^+ currents were inhibited by mibefradil with an IC_{50} around $1 \mu\text{M}$ (28).

Interestingly, the apparent potency of mibefradil depends on both the charge carrier used to record the currents and its concentration. Its sensitivity is lower in Ba^{2+} than in Ca^{2+} (29) and lower at higher divalent concentrations. For example, its potency decreases 4.5- to 9-fold by increasing the charge carrier concentration from 2 to 10 mM (18). These results suggest that mibefradil could be competing with permeant ions for a binding site in the channel. These observations are particularly relevant since most studies of mibefradil's block have used 10 mM charge carrier and thus have underestimated its potency (Table 1).

Studies on the mechanism of mibefradil block of T-type currents have yielded variable results. Early studies using a thyroid cancer cell line (hMTC, or TT cells) found little evidence for state-dependent block (29). Recent studies using rat cerebellar Purkinje neurons (22), pig atrial myocytes (20) or bovine adrenocortical cells (27) have conclusively demonstrated that mibefradil clearly shows higher affinity (5- to 20-fold) for partially inactivated states of the channel. This result has been confirmed using the cloned $\alpha 1\text{G}$ and $\alpha 1\text{H}$ channels (18, 30). Mibefradil was found to be fivefold more potent at potentials where half the channels are inactivated (18). A possible reason this effect was not observed in hMTC cells was that the measured currents were con-

taminated by other Ca^{2+} channels (29). To allow comparisons between studies, the values reported in Table 1 represent block of channels measured in supra-physiological concentrations of charge carrier at well-hyperpolarized potentials. It should be noted that at physiological concentrations of Ca^{2+} and membrane potentials, mibefradil blocks $\alpha 1\text{H}$ with an apparent IC_{50} of 70 nM (18), a value that is well within the range of clinically relevant concentrations. Since mibefradil also blocks L-type channels in a voltage-sensitive manner, it is difficult to discern whether T-type channel block is relevant to its anti-hypertensive effect.

Interestingly, the corollary has also been suggested: a block of T-type channels might contribute to the anti-hypertensive activity of dihydropyridines such as felodipine and to the antiarrhythmic activity of amiodarone and bepridil (31). Akaike and coworkers have extensively studied the sensitivity of neuronal T-type currents to calcium channel blockers (Table 1). The diphenylpiperazine flunarizine was the most potent. In fact, in hypothalamic neurons, they found that flunarizine was *more* potent at blocking T- than L-type currents, while nimodipine and diltiazem were equipotent (32). These studies demonstrated that many dihydropyridines blocked neuronal T-type currents at micromolar concentrations, with nicardipine being the most potent. Since early studies using $0.1 - 1 \mu\text{M}$ dihydropyridines had shown selective block of L-type channels with little block of T-type channels, these authors concluded that there was a sub-set of dihydropyridine-sensitive T-type channels. This hypothesis was supported in studies on the changes that occur in thalamic T-type currents during development (33). Similarly, felodipine displayed an apparent affinity for inactivated T-type channels of atrial myocytes of 13 nM, but only 700 nM for those of pituitary GH₃ cells (31).

Clearly the dihydropyridine structure-activity relationships of T- and L-type channel are different. This is most clearly demonstrated by the stereoisomers of Bay K8644: T-type channels are weakly blocked by micromolar concentrations of both (34), while for L-type channels, sub-micromolar concentrations of the (+) isomer effectively block the current, while the (-) isomer is an *agonist*, similar to the racemic mixture (35). Stimulation of LVA currents by Bay K8644 are very difficult to interpret directly because L-type channel gating is shifted to more negative potentials. In contrast, the stereoselectivity and potency of nifedipine was similar for both L- and T-type channels; the racemic mixture blocked T-type currents in guinea pig atrial myocytes with an IC_{50} of $0.18 \mu\text{M}$ (36).

Although the binding site for dihydropyridines is different between L- and T-type channels, the mechanism of block appears similar. Dihydropyridines appear to stabilize inactivated states of both channels, causing a negative shift in the steady-state availability curve (31, 37-39).

Flunarizine also blocks T-type channels in a voltage-dependent manner, while diltiazem and verapamil do not (39).

Antiepileptics

Epilepsy is a disorder of the nervous system characterized by neuronal hyperexcitability. There are many forms of epilepsy, and they have been broadly classified into either partial or generalized seizures. The drugs used to treat the symptoms of these disorders differ. Antiseizure drugs are thought to tip the balance between neuronal excitation and inhibition by two mechanisms: 1) by blocking Na^+ or Ca^{2+} channels, and hence limiting the sustained repetitive firing of neurons, or 2) by enhancing the activity of inhibitory neurotransmitters, notably gamma-aminobutyric acid (GABA). Despite the fact that few drugs have been systematically tested on both Na^+ and Ca^{2+} channels, a dogma has arisen that Na^+ channel blockers are useful in partial seizures, while T-type channel blockers are only useful in generalized seizures.

Table 2 provides numerous examples of blocking T-type channels by " Na^+ channel blockers." Perhaps the best studied is phenytoin, which clearly blocks both channels at therapeutic concentrations (40). The mechanisms of block are also similar, with higher affinity for inactivated states of the channel. Studies using cloned T-type channels indicated that $\text{Ca}_v3.2$ was the most sensitive, although the block was variable even in a cloned cell, suggesting that additional factors may be important for block (41).

Ethosuximide is considered the prototypical absence seizure drug that works by inhibition of T-type channels. This hypothesis was based on the finding that ethosuximide could partially block T-type currents in thalamic neurons at therapeutically relevant concentrations (42). Support for this hypothesis came from studies with related analogs (43). For one, T-type current block was also observed at therapeutically relevant concentrations of methyl-phenylsuccinimide (MPS), the active metabolite of methsuximide. MPS differs from ethosuximide by having a phenyl substituent at the 4 position rather than an ethyl group (Fig. 2). Second, no block was observed using the convulsant analog, tetra-methyl-succinimide. The sensitivity of T-type channels to MPS has been confirmed in many other

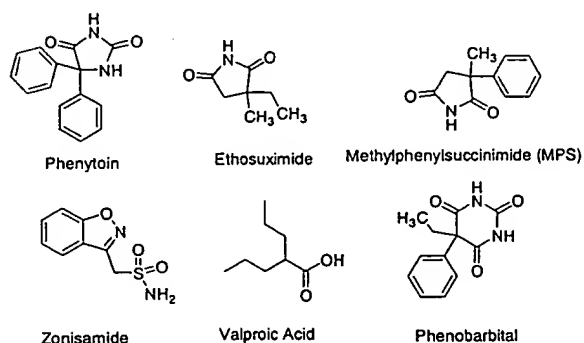


Fig. 2. Antiepileptics shown to block T-type calcium current.

Table 2. Antiepileptics shown to block T-type calcium currents

| | Phenytoin | Ethosuximide | MPS | Zonisamide | Valproate | Phenobarbital | Reference |
|------------------|-------------------|---------------|----------------|-------------------|---------------|---------------|-----------|
| | (μM) | (mM) | (mM) | (μM) | (mM) | (mM) | |
| DRG | 8 (max 58%) | 24 | 0.14 (max 42%) | | 0.3 (max 17%) | 1.7 | (41, 50) |
| DRG | | 0.007 | | | | | (44) |
| Nodose ganglion | | | | | 1 (16%) | | (91) |
| NB1 | 30 (50%) | | | 50 (38%) | | | (92) |
| Cerebral cortex | | | | 500 (60%) | | | (93) |
| Thalamus VB | 100 (33%) | 0.2 (max 40%) | 1.1 | | 1 (NE) | | (42) |
| Thalamus VB | | | 3 (52%) | | | | (94) |
| Thalamus nRT | | | 3 (53%) | | | | (94) |
| Hippocampus CA1 | 100 (43%) | | | | | | (57) |
| GH3 | 100 (36%) | 2.5 (10%) | | | | | (90) |
| $\text{Ca}_v3.1$ | 140 | 14 | 1.7 | | 3 (4%) | 1.5 | (41) |
| $\text{Ca}_v3.2$ | 8 (max 45%) | 22 | 2.3 | | 1 (9%) | | (41) |

Some compounds did not totally block the T-type current at the maximum dose tested. In such cases the values in the table represent the apparent IC_{50} with the maximum (max) block obtained in parentheses. Studies where only a single concentration was studied are noted by giving the concentration and the percent inhibition observed or NE if no significant effect was observed. The charge carrier used in each study is as follows (in mM): (reference 41) 2 Ca^{2+} , (50) 10 Ba^{2+} , (44) 1.8 Ca^{2+} , (91) 5 Ca^{2+} , (92) 51 Ba^{2+} , (93) 7 Ca^{2+} , (42) 3 Ca^{2+} , (94) 3 Ca^{2+} , (57) 10 Ca^{2+} , (90) 10 Ca^{2+} . Other abbreviations include: MPS, methylphenylsuccinimide; DRG, dorsal root ganglion; NB-1, neuroblastoma; nRT, reticular nucleus; and VB, ventrobasal.

systems, including the cloned channels (Table 2). With one notable exception (44), most studies have failed to confirm block of T-type currents at therapeutically relevant concentrations, leading to the suggestion that block of other ionic channels may be more relevant (45).

Some antiepileptics are characterized by hydantoin and imide molecular frameworks (Fig. 2). Hydantoins include phenytoin and phenobarbital and consist of a carbonyl-amine-carbonyl-amine moiety. Imides such as MPS and ethosuximide have the alternating carbonyl-amine functionality but without the additional carbonyl. It is reasonable to think that the T-channel protein would exhibit differential sensitivity to isomers of an antagonist. Such is the case with EMTBL, a cyclic thioester, where α -EMTBL exhibits blocking activity 5 times that of the β stereoisomer in rat dorsal root ganglion (DRG) (46). Chlordiazepoxide, a benzodiazepine tranquilizer that also has anti-convulsant effects, blocks both LVA and HVA channels with IC_{50} s of approximately 0.3 mM (47). Valproic acid is structurally the simplest of the antiepileptics listed in Fig. 2. Only partial block by valproic acid has been observed (Table 2). Zonisamide, a relatively new anti-epileptic, contains both a sulfonamide and oxazole functionality. It too was only capable of partial block. Based on a limited amount of experimental evidence, T-type channel block is thought to underlie the mechanism of action of both valproic acid and zonisamide.

Anesthetics

Although the precise mechanism of action of anesthetics is unknown, many studies have demonstrated that they are capable of blocking ion channels. Many general anesthetics appear to potentiate chloride currents through ligand-gated GABA and glycine channels. A newly described mechanism for inhalation anesthetics is that they hyperpolarize

neurons by potentiating the activity of leak K^+ currents carried by the two pore domain channels such as TASK-1 (48). Table 3 lists the block of T-type calcium channels by various types of anesthetics, and their structures are shown in Fig. 3.

In contrast to the tissue variability noted above, there is general agreement between studies on the potency of various inhalation anesthetics (Table 3), although decreased sensitivity of cardiac T-type currents has been noted (49). Both isoflurane and halothane block T-type currents at therapeutically relevant concentrations of anesthetics (50). Block of high voltage-activated currents by halothane occurs at similar millimolar concentrations (51, 52).

Steroid analogs have been developed that are neuroactive, including some such as alphaxalone that are anesthetic (53). New compounds have been synthesized that do not interact with GABA or Na^+ channels, such as ACN and ECN (54). It is interesting to note that of the stereoisomers of ACN and ECN, it is the (+) enantiomer of both that was most active. This suggests that the alcohol and cyano functionalities are interchangeable, since the activities (+)-ECN and (+)ACN are essentially the same despite a 'swap' of the two functional groups. T-type currents of rat DRG neurons were partially blocked by (+)-ECN (40% maximal inhibition; IC_{50} , 0.3 μ M), while (–)-ECN block occurred at 30-fold higher concentrations (54). It also produced partial block of HVA currents (approximately 30% maximal inhibition; IC_{50} , 9 μ M). Among HVA currents, (+)-ACN appears to be somewhat selective for members of the Ca_v2 family (55).

Octanol (20 μ M), an aliphatic alcohol, was reported to block LVA currents totally from inferior olivary neurons (56). Subsequent studies required much higher concentrations for block (Table 3). Studies on hippocampal CA1 pyramidal neurons indicated that octanol is non-selective,

Table 3. Anesthetics and barbiturates shown to inhibit T-type calcium currents

| | Isoflurane | Enflurane | Halothane | Pentobarbital | Thiopental | Etomidate | Propofol | Ketamine | Octanol | Reference |
|----------------------|------------|-----------|-----------|---------------|------------|-----------|------------|----------|-----------|--------------|
| | (mM) | (mM) | (mM) | (mM) | (mM) | (mM) | (μ M) | (mM) | (mM) | |
| DRG (neonatal rat) | | | 0.1 | | | | | | | (52) |
| DRG (rat) | 0.3 | 1.2 (56%) | 0.6 | 0.3 | | 0.2 | 13 | 2.5 | 0.12 | (41, 49, 50) |
| Hippocampus | 1 (75%) | | | | | | | | 0.3 (53%) | (57, 95) |
| Ventricular myocytes | 1.2 (20%) | | 1.4 (20%) | | | | | | | (49) |
| Adrenal glomerulosa | 0.7 (47%) | 1.2 (56%) | 0.7 (24%) | | | | | | | (49) |
| GH3 | | | 1.3 | 1 | | | | | 0.24 | (51, 90) |
| Thyroid carcinoma | 0.7 (33%) | 1.2 (46%) | 0.7 (24%) | | | | | | | (49, 96) |
| Ca _v 3.1 | 0.3 | | | 0.3 | 0.3 | 0.16 | 20 | 1.2 | 0.16 | (41) |
| Ca _v 3.2 | | | | 0.3 | | | 27 | | 0.22 | (41) |

The values represent either the IC_{50} determined from dose-response measurements or the percent inhibition (in parentheses) by a single concentration. The charge carrier used in each study is as follows (mM): (reference 52) 10 Ca^{2+} ; (41) 2 Ca^{2+} ; (49) adrenal glomerulosa: 20 Ca^{2+} ; DRG: 2 Ca^{2+} ; thyroid: 10 Ca^{2+} ; ventricular myocyte: 2 Ca^{2+} ; (50) 10 Ba^{2+} ; (57) 2 Ca^{2+} ; (95) 5 Ca^{2+} ; (51), 10 Ca^{2+} ; (90) 10 Ca^{2+} ; (96) 10 Ca^{2+} .

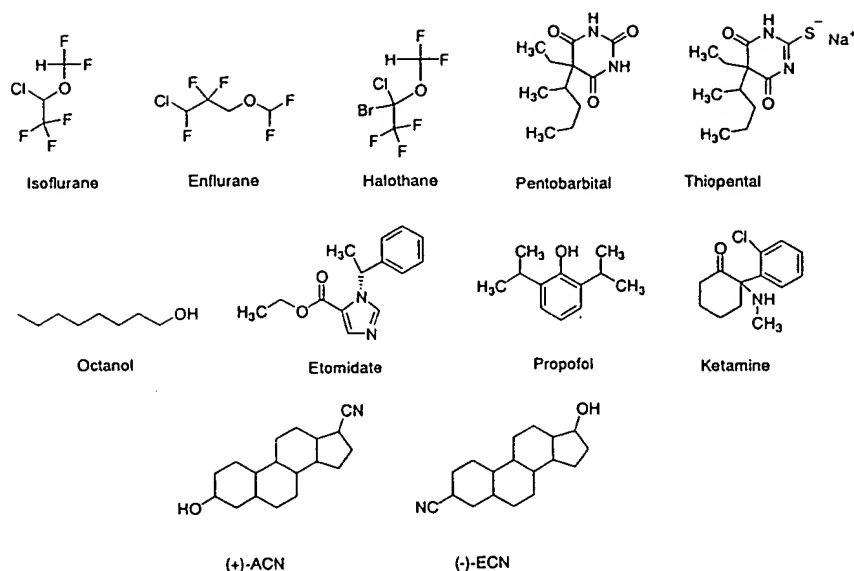


Fig. 3. Anesthetics shown to block T-type calcium current.

blocking T-, N- and L-type channels to a similar extent (57).

Antipsychotics

Antipsychotics, introduced in the 1950s, are used today in the treatment of psychotic disorders such as schizophrenia, the main phase of manic-depressive illness and other acute idiopathic psychotic illnesses (58). Anti-psychotics (neuroleptics) primarily act to block the D2 dopaminergic receptors, thereby inactivating dopamine neurotransmission in the forebrain. In addition, some neuroleptics can act on the D1 dopaminergic, 5-HT₂ serotonergic and α_2 -adrenergic receptors (59).

The antipsychotics shown in Fig. 4 are characterized by varying degrees of aromaticity, and heterocyclic, non-aliphatic amines. The core amine heterocycles are all 1,4 di-substituted. Five of the six compounds have halogens (chlorine and fluorine) on the aromatic rings located primarily at the *para* position. With the exception of clozapine, all these compounds have short (2–3) carbon aliphatic chains connecting the heterocyclic amines to the aromatic rings. The most structurally similar compounds are penfluridol, fluspirilene and pimozide. The higher sensitivity of T-type channels to penfluridol might be attributed to a decrease in steric bulk and hydrogen bonding ability of the hydroxyl at the 4 position compared to the others. Despite strikingly different structures, thioridazine, clozapine and haloperidol have comparable activity in TT cells, but are still much less active than fluspirilene or penfluridol (60).

Of the three diphenylbutylpiperidines, penfluridol was

the most effective at blocking T-type currents of human medullary thyroid cancer (TT) cells (60). In these cells, penfluridol blocked with an IC₅₀ of 224 nM. It was also approximately tenfold more selective for LVA currents over HVA currents as 500 nM penfluridol inhibited 82% of the LVA current but only 20% of the HVA. Both penfluridol and pimozide block in a state-dependent manner, consistent with a lower affinity to the resting state (60, 61). Of all the compounds tested on T-type currents, these are the only class of drugs with IC₅₀'s in the sub-micromolar range (Table 4). Unfortunately, they are also very potent blockers of K⁺ channels (26) and bind tightly to L-type channels (62).

Others

Amiloride is a potassium-sparing diuretic that acts by blocking a *non-voltage-activated* Na⁺ channel in kidney epithelial cells (ENaC). It can also block voltage-gated channels, preferentially blocking LVA currents with little block of HVA channels or voltage-activated Na⁺ channels (63). Studies using cardiac myocytes have confirmed the selectivity of amiloride for T- vs L-type channels (64, 65). Its selectivity for LVA currents has been a useful tool in a number of studies on neuronal Ca²⁺ currents (66). In contrast, most studies have not confirmed amiloride's sensitivity, requiring up to 30-fold higher concentrations (Table 5). Although this discrepancy might be explained by differential sensitivity of the T-type channel subtypes (67, 68), it does not explain discrepancies between studies on the same cell type. For example, using mouse spermato-

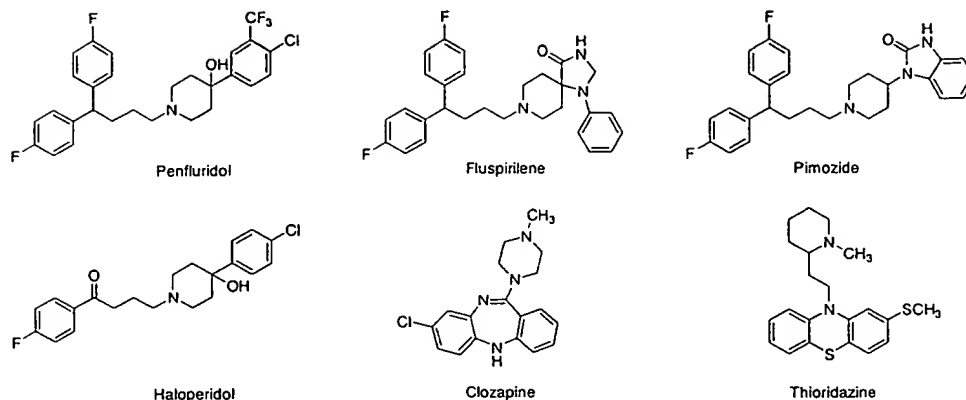


Fig. 4. Antipsychotics shown to inhibit T-type calcium channel activity.

Table 4. Antipsychotics shown to inhibit T-type calcium channel activity

| | Penfluridol | Fluspirilene | Clozapine | Haloperidol | Thioridazine | Pimozide | Reference |
|---------------------------|-------------|--------------|-----------|-------------|--------------|----------|-----------|
| Pituitary (rat)-GH4C1 | 1 (45%) | 2 (64%) | | | | | (97) |
| Thyroid carcinoma (rat) | 0.2 | | | | | | (60) |
| Thyroid carcinoma (human) | 0.1 (70%) | 1 (90%) | 10 | 5 (31%) | 10 (25%) | | (60) |
| Spermatocytes (mouse) | | | | | | 0.5 | (61) |

All concentrations reported are micromolar and represent the IC_{50} values determined from dose-response measurements. Studies where only a single concentration was studied are noted by giving the concentration and the percent inhibition observed. The charge carrier used in each study is as follows (mM): (reference 97) 5 Ca^{2+} , (60) 10 Ca^{2+} , (61) 10 Ca^{2+} .

genic cells, Santi and co-workers (69) found that 0.5 mM amiloride only blocked 62% of the T-type current, while Arnoult et al. found that roughly half this concentration produced half-maximal block, reporting an IC_{50} of 0.24 mM (17). In addition to blocking ENaC channels, the usefulness of millimolar concentrations of amiloride is further limited by its block of transporters, such as the Na^+/H^+ and Na^+/Ca^{2+} transporters (70).

It has been hypothesized that blockade of T-type channels may provide a neuroprotective effect after ischemia (71, 72). To this end, a number of dimethylphenyl-piperazines (e.g., U-92032 (73)) and arylpiperidine analogs (e.g., SUN N5030 (72)) have been evaluated (Fig. 5). Although analogs have been described that are selective for LVA over HVA channels, they block voltage-gated Na^+ channels at similar concentrations. Similarly, the lamotrigine analog sipatrigine is a neuroprotective agent, is capable of blocking T-type channels, and can block Na^+ channels (74).

Tetrandrine, a plant alkaloid isolated from the root of *Stephania tetrandra*, was equally effective at blocking T-channels in adrenal glomerulosa cells, Y_1 adrenocortical tumor cells and bullfrog cardiomyocytes at approximately 10 μ M (Table 5). It also blocks L-type channels at similar concentrations (75).

In contrast to their potent effects on HVA channels, a

selective peptide toxin for LVA channels has yet to be isolated from either spider or snail toxins. A scorpion toxin was isolated that appeared to be selective for LVA channels, since 350 nM could block currents through cloned T-type channels with no effect on the cloned HVA channels $Ca_v1.2$, $Ca_v2.1$, $Ca_v2.2$ and $Ca_v2.3$ (76). Unfortunately its usefulness is limited by its ability to modify gating of Na^+ channels.

Conclusions

Because T-type calcium currents have been found in a variety of tissue and cell types, many physiological and pathophysiological functions for the channel have been proposed. T-type channels are most abundant in neurons, especially in medium-sized neurons from sensory ganglia (77). T-type currents have also been recorded from smooth muscle myocytes, pancreatic β cells, adrenocortical cells, osteoblasts, fibroblasts and glial cells (13). Physiological roles for the T-type channel include smooth muscle contraction, hormone (but not neurotransmitter) secretion and regulation of neuronal excitability, where they mediate rebound burst firing (13, 78). Increased T-type channel expression has been observed in proliferating and hypertrophic myocytes, leading to the hypothesis that they may also be involved in cell cycle progression (reviewed in

Table 5. Other compounds shown to block T-type calcium channels

| | Amiloride | U-92032 | Tetrandrine | Reference |
|------------------------|------------|---------|---------------|-----------|
| | mM | μ M | μ M | |
| DRG (chick) | 0.03 | | | (63) |
| DRG (rat) | 0.076 | | | (50) |
| Motoneuron | 1 (74%) | | | (21) |
| Neuroblastoma, N18 | 0.03 | | | (63) |
| Neuroblastoma, N1E-115 | | 6 (50%) | 2.5 (max 70%) | (73, 88) |
| Neuroblastoma, IMR-32 | 0.5 (58%) | | | (98) |
| Thalamus nRT | 0.5 (41%) | | | (94) |
| Thalamus VB | 0.5 (38%) | | | (94) |
| Hippocampus CA1 | 0.3 (43%) | 0.5 | | (57, 99) |
| Atrial myocytes | | 1 | | (100) |
| Ventricular myocytes | 0.23 | | 10 (57%) | (64, 75) |
| Cardiac Purkinje | 0.25 (50%) | | | (65) |
| GH3 | 1.55 | | | (90) |
| Spermatocytes | 0.24 | | | (61) |
| Ca _v 3.2 | 0.17 | | | (67) |

The charge carrier used in each study is as follows (in mM): (reference 63) 5 Ca²⁺, (50) 10 Ba²⁺, (21) 5 Ba²⁺, (73) 50 Ba²⁺, (88) 20 Ba²⁺, (98) 10 Ca²⁺, (94) 3 Ca²⁺, (57) 10 Ca²⁺, (99) 2 Ca²⁺, (100) 5 Ca²⁺, (64) 5.4 Ca²⁺, (75) 1.8 Ca²⁺, (65) 5 Ca²⁺, (90) 10 Ca²⁺, (61) 10 Ca²⁺, (67) 15 Ba²⁺. Abbreviations: DRG, dorsal root ganglion; N1E-115, mouse neuroblastoma; nRT, reticular nucleus; VB, ventrobasal.

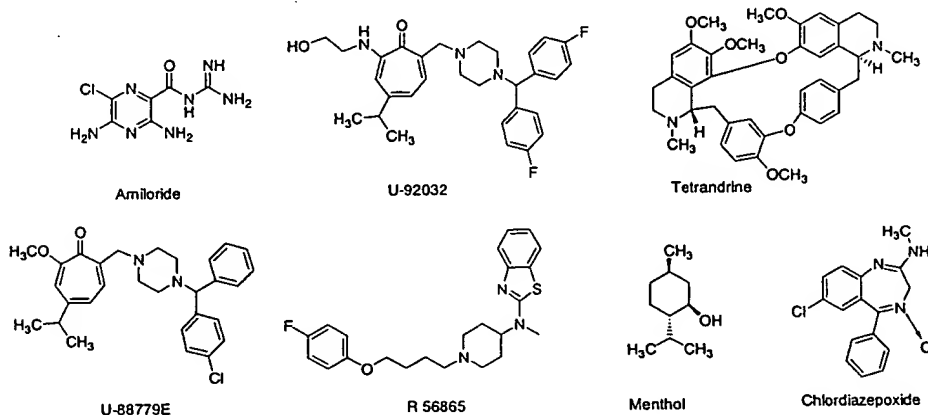


Fig. 5. A variety of structurally diverse compounds that block T-type calcium current.

ref. 13). Although to date there are no highly selective T-type channel blockers, studies using a variety of compounds that all have activity against these channels have led to the conclusion that selective blockers might be useful in regulating proliferation, blood pressure and abnormal neuronal firing. T-type channels may play a central role in thalamic dysrhythmias and therefore blockers may be useful not only against epilepsy but also a wide spectrum of neurological disorders (79). The clinical observation that high doses of anti-epileptics are analgesic, coupled with the observation that sensory neurons contain large T-type currents, leads to the speculation that a T-type channel drug

may be useful in the treatment of neuropathic pain (80). It is important to note that in many neurons, T-type channels may serve as pacemaker currents, depolarizing the membrane to a level where Na⁺ channels may fire. In these cases, there is a "pharmacological amplification" (81) of T-type channel inhibition such that even 10% block may lead to a pronounced effect on neuronal firing (82). It should also be noted that selectivity for T-type channels may be conferred by a drug's preference for inactivated channels. This may be particularly true in thalamic dysrhythmias since T-type channels are partially inactivated in states of wakefulness (83).

REFERENCES

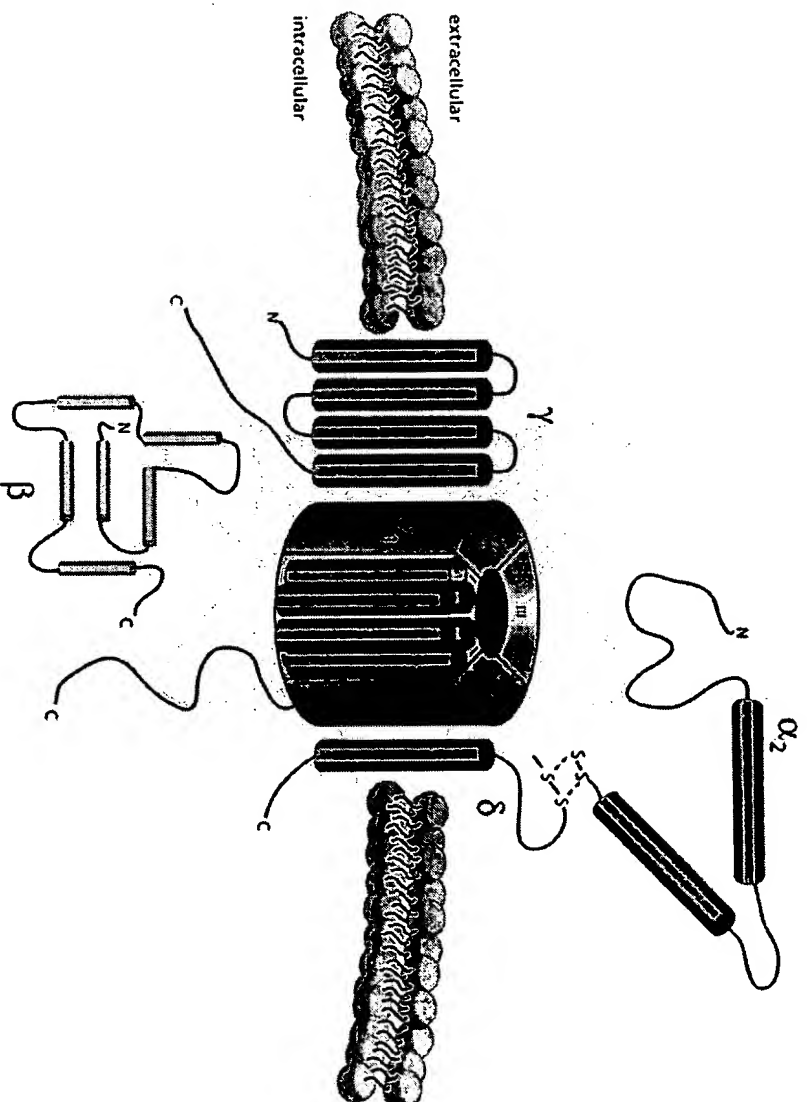
- Randall A and Tsien RW: Pharmacological dissection of multiple types of Ca^{2+} channel currents in rat cerebellar granule neurons. *J Neurosci* 15, 2995–3012 (1995)
- Olivera BM, Miljanich GP, Ramachandran J and Adams ME: Calcium channel diversity and neurotransmitter release: the ω -conotoxins and ω -agatoxins. *Annu Rev Biochem* 63, 823–867 (1994)
- Ertel E, Campbell K, Harpold MM, Hofmann F, Mori Y, Perez-Reyes E, Schwartz A, Snutch T, Tanabe T, Birnbaumer L, Tsien RW and Catterall WA: Nomenclature of voltage-gated calcium channels. *Neuron* 25, 533–535 (2000)
- Doyle DA, Cabral JM, Pfuetzner RA, Kuo A, Gulbis JM, Cohen SL, Chait BT and MacKinnon R: The structure of the potassium channel: molecular basis of K^{+} conduction and selectivity. *Science* 280, 69–77 (1998)
- Huber I, Wapfel E, Herzog A, Mitterdorfer J, Glossmann H, Langer T and Striessnig J: Conserved Ca^{2+} -antagonist-binding properties and putative folding structure of a recombinant high-affinity dihydropyridine-binding domain. *Biochem J* 347 Pt 3, 829–836 (2000)
- Hofmann F, Lacinova L and Klugbauer N: Voltage-dependent calcium channels: from structure to function. *Rev Physiol Biochem Pharmacol* 139, 33–87 (1999)
- Klugbauer N, Dai S, Specht V, Lacinova L, Marais E, Bohn G and Hofmann F: A family of γ -like calcium channel subunits. *FEBS Lett* 470, 189–197 (2000)
- Wei X, Pan S, Lang W, Kim H, Schneider T, Perez-Reyes E and Birnbaumer L: Molecular determinants of cardiac Ca^{2+} channel pharmacology: subunit requirement for the high affinity and allosteric regulation of dihydropyridine binding. *J Biol Chem* 270, 27106–27111 (1995)
- Gee NS, Brown JP, Dissanayake VUK, Offord J, Thurlow R and Woodruff GN: The novel anticonvulsant drug, gabapentin (Neurontin) binds to the $\alpha_2\delta$ subunit of a calcium channel. *J Biol Chem* 271, 5768–5776 (1996)
- Abernethy DR and Schwartz JB: Drug therapy: calcium-antagonist drugs. *N Engl J Med* 341, 1447–1457 (1999)
- Triggle DJ: The pharmacology of ion channels: with particular reference to voltage-gated Ca^{2+} channels. *Eur J Pharmacol* 375, 311–325 (1999)
- Welling A, Ludwig A, Zimmer S, Klugbauer N, Flockerzi V and Hofmann F: Alternatively spliced IS6 segments of the $\alpha_1\text{C}$ gene determine the tissue-specific dihydropyridine sensitivity of cardiac and vascular smooth muscle L-type Ca^{2+} channels. *Circ Res* 81, 526–532 (1997)
- Ertel SI, Ertel EA and Clozel JP: T-type Ca^{2+} channels and pharmacological blockade: potential pathophysiological relevance. *Cardiovasc Drugs Ther* 11, 723–739 (1997)
- Mishra SK and Hermsmeider K: Selective inhibition of T-type Ca^{2+} channels by Ro 40-5967. *Circ Res* 75, 144–148 (1994)
- Benardeau A and Ertel E: Selective block of myocardial T-type calcium channels by mibefradil: A comparison with the 1,4-dihydropyridine, amlodipine. In *Selective Block of Myocardial T-type Calcium Channels by Mibefradil: A Comparison with the 1,4-Dihydropyridine, Amlodipine*, Edited by Clozel JP, Nargeot J and Tsien RW, pp 386–394, Adis International Chester, UK (1997)
- Kobrin I, Bieska G, Charlton V, Lindberg E and Pordy R: Anti-anginal and anti-ischemic effects of mibefradil, a new T-type calcium channel antagonist. *Cardiology* 89, 23–32 (1998)
- Arnoult C, Lemons JR and Florman HM: Voltage-dependent modulation of T-type calcium channels by protein tyrosine phosphorylation. *EMBO J* 16, 1593–1599 (1997)
- Martin RL, Lee JH, Cribbs LL, Perez-Reyes E and Hanck DA: Mibefradil block of cloned T-type calcium channels. *J Pharmacol Exp Ther* 295, 302–308 (2000)
- Monteil A, Chemin J, Leuranguer V, Altier C, Mennessier G, Bourinet E, Lory P and Nargeot J: Specific properties of T-type calcium channels generated by the human $\alpha_1\text{I}$ subunit. *J Biol Chem* 275, 16530–16535 (2000)
- Perchenet L, Benardeau A and Ertel EA: Pharmacological properties of $\text{Ca}_v3.2$, a low voltage-activated Ca^{2+} channel cloned from human heart. *Naunyn Schmiedeberg's Arch Pharmacol* 361, 590–599 (2000)
- Viana F, Van den Bosch L, Missiaen L, Vandenberghe W, Droogmans G, Nilius B and Robberecht W: Mibefradil (Ro 40-5967) blocks multiple types of voltage-gated calcium channels in cultured rat spinal motoneurons. *Cell Calcium* 22, 299–311 (1997)
- McDonough SI and Bean BP: Mibefradil inhibition of T-type calcium channels in cerebellar Purkinje neurons. *Mol Pharmacol* 54, 1080–1087 (1998)
- Bezprozvanny I and Tsien RW: Voltage-dependent blockade of diverse types of voltage-gated Ca^{2+} channels expressed in *Xenopus* oocytes by the Ca^{2+} channel antagonist mibefradil (Ro 40-5967). *Mol Pharmacol* 48, 540–549 (1995)
- Nilius B, Prenen J, Kamouchi M, Viana F, Voets T and Droogmans G: Inhibition by mibefradil, a novel calcium channel antagonist, of Ca^{2+} - and volume-activated Cl^{-} channels in macrovascular endothelial cells. *Br J Pharmacol* 121, 547–555 (1997)
- Liu JH, Bijlenga P, Occhiodoro T, Fischer-Lougheed J, Bader CR and Bernheim L: Mibefradil (Ro 40-5967) inhibits several Ca^{2+} and K^{+} currents in human fusion-competent myoblasts. *Br J Pharmacol* 126, 245–250 (1999)
- Gomora JC and Enyeart JJ: Dual pharmacological properties of a cyclic AMP-sensitive potassium channel. *J Pharmacol Exp Ther* 290, 266–275 (1999)
- Gomora JC, Xu L, Enyeart JA and Enyeart JJ: Effect of mibefradil on voltage-dependent gating and kinetics of T-type Ca^{2+} channels in cortisol-secreting cells. *J Pharmacol Exp Ther* 292, 96–103 (2000)
- Eller P, Berjukov S, Wanner S, Huber I, Hering S, Knaus HG, Toth G, Kimball SD and Striessnig J: High affinity interaction of mibefradil with voltage-gated calcium and sodium channels. *Br J Pharmacol* 130, 669–677 (2000)
- Mehrke G, Zong XG, Flockerzi V and Hofmann F: The Ca^{2+} -channel blocker Ro 40-5967 blocks differently T-type and L-type Ca^{2+} channels. *J Pharmacol Exp Ther* 271, 1483–1488 (1994)
- Klugbauer N, Marais E, Lacinova L and Hofmann F: A T-type calcium channel from mouse brain. *Pflügers Arch* 437, 710–715 (1999)
- Cohen CJ, Spires S and Van Skiver D: Block of T-type Ca channels in guinea pig atrial cells by antiarrhythmic agents and Ca channel antagonists. *J Gen Physiol* 100, 703–728 (1992)
- Akaike N, Kostyuk PG and Osipchuk YV: Dihydropyridine-sensitive low-threshold calcium channels in isolated rat hypo-

- thalamic neurones. *J Physiol (Lond)* **412**, 181 – 195 (1989)
- 33 Tarasenko AN, Kostyuk PG, Eremin AV and Isaev DS: Two types of low-voltage-activated Ca^{2+} channels in neurones of rat laterodorsal thalamic nucleus. *J Physiol (Lond)* **499**, 77 – 86 (1997)
 - 34 Lievano A, Bolden A and Horn R: Calcium channels in excitable cells: divergent genotypic and phenotypic expression of α_1 -subunits. *Am J Physiol* **267**, C411 – C424 (1994)
 - 35 Kass RS: Voltage-dependent modulation of cardiac calcium channel current by optical isomers of Bay K 8644: implications for channel gating. *Circ Res* **61**, 11 – 15 (1987)
 - 36 Romanin C, Seydl K, Glossmann H and Schindler H: The dihydropyridine nifedipine inhibits T-type Ca^{2+} currents in atrial myocytes. *Pflügers Arch* **420**, 410 – 412 (1992)
 - 37 Bean BP: Nitrendipine block of cardiac calcium channels: high-affinity binding to the inactivated state. *Proc Natl Acad Sci USA* **81**, 6388 – 6392 (1984)
 - 38 Richard S, Diochot S, Nargeot J, Baldy-Moulinier and Valmier J: Inhibition of T-type calcium currents by dihydropyridines in mouse embryonic dorsal root ganglion neurons. *Neurosci Lett* **132**, 229 – 234 (1991)
 - 39 Kuga T, Sadoshima J, Tomoike H, Kanaide H, Akaïke N and Nakamura M: Actions of Ca^{2+} antagonists on two types of Ca^{2+} channels in rat aorta smooth muscle cells in primary culture. *Circ Res* **67**, 469 – 480 (1990)
 - 40 Twombly DA, Yoshi M and Narahashhi T: Mechanisms of calcium channel block by phenytoin. *J Pharmacol Exp Ther* **246**, 189 – 195 (1988)
 - 41 Todorovic SM, Perez-Reyes E and Lingle CJ: Anticonvulsants but not general anesthetics have differential blocking effects on different T-type current variants. *Mol Pharmacol* **58**, 98 – 108 (2000)
 - 42 Coulter DA, Huguenard JR and Prince DA: Characterization of ethosuximide reduction of low-threshold calcium current in thalamic neurons. *Ann Neurol* **25**, 582 – 593 (1989)
 - 43 Coulter DA, Huguenard JR and Prince DA: Differential effects of petit mal anticonvulsants and convulsants on thalamic neurones: calcium current reduction. *Br J Pharmacol* **100**, 800 – 806 (1990)
 - 44 Kostyuk PG, Molokanova EA, Pronchuk NF, Savchenko AN and Verkhatsky AN: Different action of ethosuximide on low- and high-threshold calcium currents in rat sensory neurons. *Neuroscience* **51**, 755 – 758 (1992)
 - 45 Leresche N, Parri HR, Erdemli G, Guyon A, Turner JP, Williams SR, Asprohini E and Crunelli V: On the action of the anti-absence drug ethosuximide in the rat and cat thalamus. *J Neurosci* **18**, 4842 – 4853 (1998)
 - 46 Gross RA, Covey DF and Ferrendelli JA: Voltage-dependent calcium channels as targets for convulsant and anticonvulsant alkyl-substituted thiobutyrolactones. *J Pharmacol Exp Ther* **280**, 686 – 694 (1997)
 - 47 Reuveny E, Twombly DA and Narahashi T: Chlordiazepoxide block of two types of calcium channels in neuroblastoma cells. *J Pharmacol Exp Ther* **264**, 22 – 28 (1993)
 - 48 Sirois JE, Lei Q, Talley EM, Lynch C 3rd and Bayliss DA: The TASK-1 two-pore domain K^+ channel is a molecular substrate for neuronal effects of inhalation anesthetics. *J Neurosci* **20**, 6347 – 6354 (2000)
 - 49 McDowell TS, Pancrazio JJ, Barrett PQ and Lynch C 3rd: Volatile anesthetic sensitivity of T-type calcium currents in various cell types. *Anesth Analg* **88**, 168 – 173 (1999)
 - 50 Todorovic SM and Lingle CJ: Pharmacological properties of T-type Ca^{2+} current in adult rat sensory neurons: effects of anticonvulsant and anesthetic agents. *J Neurophysiol* **79**, 240 – 252 (1998)
 - 51 Herrington J, Stern RC, Evers AS and Lingle CJ: Halothane inhibits two components of calcium current in clonal (GH3) pituitary cells. *J Neurosci* **11**, 2226 – 2240 (1991)
 - 52 Takenoshita M and Steinbach JH: Halothane blocks low-voltage-activated calcium currents in rat sensory neurons. *J Neurosci* **11**, 1404 – 1412 (1991)
 - 53 Gasior M, Carter RB and Witkin JM: Neuroactive steroids: potential therapeutic use in neurological and psychiatric disorders. *Trends Pharmacol Sci* **20**, 107 – 112 (1999)
 - 54 Todorovic SM, Prakriya M, Nakashima YM, Nilsson KR, Han M, Zorumski CF, Covey DF and Lingle CJ: Enantioselective blockade of T-type Ca^{2+} current in adult rat sensory neurons by a steroid that lacks gamma-aminobutyric acid-modulatory activity. *Mol Pharmacol* **54**, 918 – 927 (1998)
 - 55 Nakashima YM, Todorovic SM, Covey DF and Lingle CJ: The anesthetic steroid (+)-3 α -hydroxy-5 α -androstane-17 β -carbonitrile blocks N-, Q-, and R-type, but not L- and P-type, high voltage-activated Ca^{2+} current in hippocampal and dorsal root ganglion neurons of the rat. *Mol Pharmacol* **54**, 559 – 568 (1998)
 - 56 Llinas RR: The intrinsic electrophysiological properties of mammalian neurons: insights into central nervous system function. *Science* **242**, 1654 – 1664 (1988)
 - 57 Takahashi K, Wakamori M and Akaïke N: Hippocampal CA1 pyramidal cells of rats have four voltage-dependent calcium conductances. *Neurosci Lett* **104**, 229 – 234 (1989)
 - 58 Baldessarini RJ: Drugs and the treatment of psychiatric disorders. *In* *Drugs and the Treatment of Psychiatric Disorders*, Edited by Hardman JG, Limbird LE, Molinoff PB, Ruddon RW and Gilman AG, pp 399 – 430, McGraw-Hill, New York (1996)
 - 59 Hardman JG, Limbird LE, Molinoff PB, Ruddon RW and Gilman AG: *In* *The Pharmacological Basis of Therapeutics*, pp 1 – 1905, McGraw-Hill, New York (1996)
 - 60 Enyeart JJ, Biagi BA and Mlinar B: Preferential block of T-type calcium channels by neuroleptics in neural crest-derived rat and human C cell lines. *Mol Pharmacol* **42**, 364 – 372 (1992)
 - 61 Arnoult C, Villaz M and Florman HM: Pharmacological properties of the T-type Ca^{2+} current of mouse spermatogenic cells. *Mol Pharmacol* **53**, 1104 – 1111 (1998)
 - 62 King VF, Garcia ML, Shevell JL, Slaughter RS and Kaczorowski GJ: Substituted diphenylbutylpiperidines bind to a unique high affinity site on the L-type calcium channel. Evidence for a fourth site in the cardiac calcium entry blocker receptor complex. *J Biol Chem* **264**, 5633 – 5641 (1989)
 - 63 Tang C-M, Presser F and Morad M: Amiloride selectively blocks the low threshold (T) calcium channel. *Science* **240**, 213 – 215 (1988)
 - 64 Tytgat J, Vereecke J and Carmeliet E: Mechanism of cardiac T-type Ca channel blockade by amiloride. *J Pharmacol Exp Ther* **254**, 546 – 551 (1990)
 - 65 Hirano Y, Fozzard HA and January CT: Characteristics of L- and T-type Ca^{2+} currents in canine cardiac Purkinje cells. *Am J Physiol* **256**, H1478 – H1492 (1989)
 - 66 McCobb DP and Beam KG: Action potential waveform voltage-clamp commands reveal striking differences in calcium entry via low and high voltage-activated calcium channels. *Neuron* **7**,

- 119–127 (1991)
- 67 Williams ME, Washburn MS, Hans M, Urrutia A, Brust PF, Prodanovich P, Harpold MM and Stauderman KA: Structure and functional characterization of a novel human low-voltage activated calcium channel. *J Neurochem* 72, 791–799 (1999)
- 68 Monteil A, Chemin J, Bourinet E, Mennessier G, Lory P and Nargeot J: Molecular and functional properties of the human $\alpha 1G$ subunit that forms T-type calcium channels. *J Biol Chem* 275, 6090–6100 (2000)
- 69 Santi CM, Darszon A and Hernandez-Cruz A: A dihydropyridine-sensitive T-type Ca^{2+} current is the main Ca^{2+} current carrier in mouse primary spermatocytes. *Am J Physiol* 271, C1583–C1593 (1996)
- 70 Kleyman TR and Cragoe EJ Jr.: Amiloride and its analogs as tools in the study of ion transport. *J Membr Biol* 105, 1–21 (1988)
- 71 Im HK, Im WB and Tsuzuki K: Selective block of transient Ca channel current in mouse neuroblastoma cells by U-88779E. *J Pharmacol Exp Ther* 265, 529–535 (1993)
- 72 Annoura H, Nakanishi K, Uesugi M, Fukunaga A, Miyajima A, Tamura-Horikawa Y and Tamura S: A novel class of Na^+ and Ca^{2+} channel dual blockers with highly potent anti-ischemic effects. *Bioorg Med Chem Lett* 9, 2999–3002 (1999)
- 73 Ito C, Im WB, Takagi H, Takahashi M, Tsuzuki K, Liou SY and Kuniyama H: U-92032, a T-type Ca^{2+} channel blocker and antioxidant, reduces neuronal ischemic injuries. *Eur J Pharmacol* 257, 203–210 (1994)
- 74 McNaughton NC, Hainsworth AH, Green PJ and Randall AD: Inhibition of recombinant low-voltage-activated Ca^{2+} channels by the neuroprotective agent BW619C89 (Sipatrigine). *Neuropharmacology* 39, 1247–1253 (2000)
- 75 Rubio LS, Garrido G, Llanes L and Alvarez JL: Effects of tetrandrine on Ca^{2+} - and Na^+ -currents of single bullfrog cardiomyocytes. *J Mol Cell Card* 25, 801–813 (1993)
- 76 Chuang RS, Jaffe H, Cribbs L, Perez-Reyes E and Swartz KJ: Inhibition of T-type voltage-gated calcium channels by a new scorpion toxin. *Nat Neurosci* 1, 668–674 (1998)
- 77 Scroggs RS and Fox AP: Calcium current variation between acutely isolated adult rat dorsal root ganglion neurons of different size. *J Physiol (Lond)* 445, 639–658 (1992)
- 78 Huguenard JR: Low threshold calcium currents in central nervous system neurons. *Annu Rev Physiol* 58, 329–348 (1996)
- 79 Llinas RR, Ribary U, Jeanmonod D, Kronberg E and Mitra PP: Thalamocortical dysrhythmia: A neurological and neuropsychiatric syndrome characterized by magnetoencephalography. *Proc Natl Acad Sci USA* 96, 15222–15227 (1999)
- 80 McQuay H, Carroll D, Jadad AR, Wiffen P and Moore A: Anticonvulsant drugs for management of pain: a systematic review. *Br Med J* 311, 1047–1052 (1995)
- 81 Narahashi T: Neuroreceptors and ion channels as the basis for drug action: past, present, and future. *J Pharmacol Exp Ther* 294, 1–26 (2000)
- 82 Huguenard JR and Prince DA: Intrathalamic rhythmicity studied in vitro: nominal T-current modulation causes robust antioscillatory effects. *J Neurosci* 14, 5485–5502 (1994)
- 83 McCormick DA and Bal T: Sleep and arousal: thalamocortical mechanisms. *Annu Rev Neurosci* 20, 185–215 (1997)
- 84 Kaneda M and Akaike N: The low-threshold Ca current in isolated amygdaloid neurons in the rat. *Brain Res* 497, 187–190 (1989)
- 85 Takahashi K and Akaike N: Calcium antagonist effects on low-threshold (T-type) calcium current in rat isolated hippocampal CA1 pyramidal neurons. *J Pharmacol Exp Ther* 256, 169–175 (1991)
- 86 Liu Y and Lasater EM: Calcium currents in turtle retinal ganglion cells. I. The properties of T- and L-type currents. *J Neurophysiol* 71, 733–742 (1994)
- 87 Randall AD and Tsien RW: Contrasting biophysical and pharmacological properties of T-type and R-type calcium channels. *Neuropharmacology* 36, 879–893 (1997)
- 88 Liu Y, Karpinski E, Rao MR and Pang PKT: Tetrandrine: a novel calcium channel antagonist inhibits type I calcium channels in neuroblastoma cells. *Neuropharmacology* 30, 1325–1331 (1991)
- 89 Tytgat J, Vereecke J and Carmeliet E: Mechanism of L- and T-type Ca^{2+} channel blockade by flunarizine in ventricular myocytes of the guinea-pig. *Eur J Pharmacol* 296, 189–197 (1996)
- 90 Herrington J and Lingle CJ: Kinetic and pharmacological properties of low voltage-activated Ca^{2+} current in rat clonal (GH3) pituitary cells. *J Neurophysiol* 68, 213–232 (1992)
- 91 Kelly KM, Gross RA and Macdonald RL: Valproic acid selectively reduces the low-threshold (T) calcium current in rat nodose neurons. *Neurosci Lett* 116, 233–238 (1990)
- 92 Kito M, Maehara M and Watanabe K: Mechanisms of T-type calcium channel blockade by zonisamide. *Seizure* 5, 115–119 (1996)
- 93 Suzuki S, Kawakami K, Nishimura S, Watanabe Y, Yagi K, Seino M and Miyamoto K: Zonisamide blocks T-type calcium channel in cultured neurons of rat cerebral cortex. *Epilepsy Res* 12, 21–27 (1992)
- 94 Huguenard JR and Prince DA: A novel T-type current underlies prolonged Ca^{2+} -dependent burst firing in GABAergic neurons of rat thalamic reticular nucleus. *J Neurosci* 12, 3804–3817 (1992)
- 95 Study RE: Isoflurane inhibits multiple voltage-gated calcium currents in hippocampal pyramidal neurons. *Anesthesiology* 81, 104–116 (1994)
- 96 McDowell TS, Pancrazio JJ and Lynch C 3rd: Volatile anesthetics reduce low-voltage-activated calcium currents in a thyroid C-cell line. *Anesthesiology* 85, 1167–1175 (1996)
- 97 Enyeart JJ, Biagi BA, Day RN, Sheu SS and Maurer RA: Blockade of low and high threshold Ca^{2+} channels by diphenylbutylpiperidine antipsychotics linked to inhibition of prolactin gene expression. *J Biol Chem* 265, 16373–16379 (1990)
- 98 Carbone E, Sher E and Clementi F: Ca currents in human neuroblastoma IMR32 cells: kinetics, permeability, and pharmacology. *Pflügers Arch* 416, 170–179 (1990)
- 99 Avery RB and Johnston D: Ca^{2+} channel antagonist U-92032 inhibits both T-type Ca^{2+} channels and Na^+ channels in hippocampal CA1 pyramidal neurons. *J Neurophysiol* 77, 1023–1028 (1997)
- 100 Xu X and Lee KS: A selective blocker for rested T-type Ca^{2+} channels in guinea pig atrial cells. *J Pharmacol Exp Ther* 268, 1135–1142 (1994)

Voltage-Gated Calcium Channels

SIGMA-ALDRICH



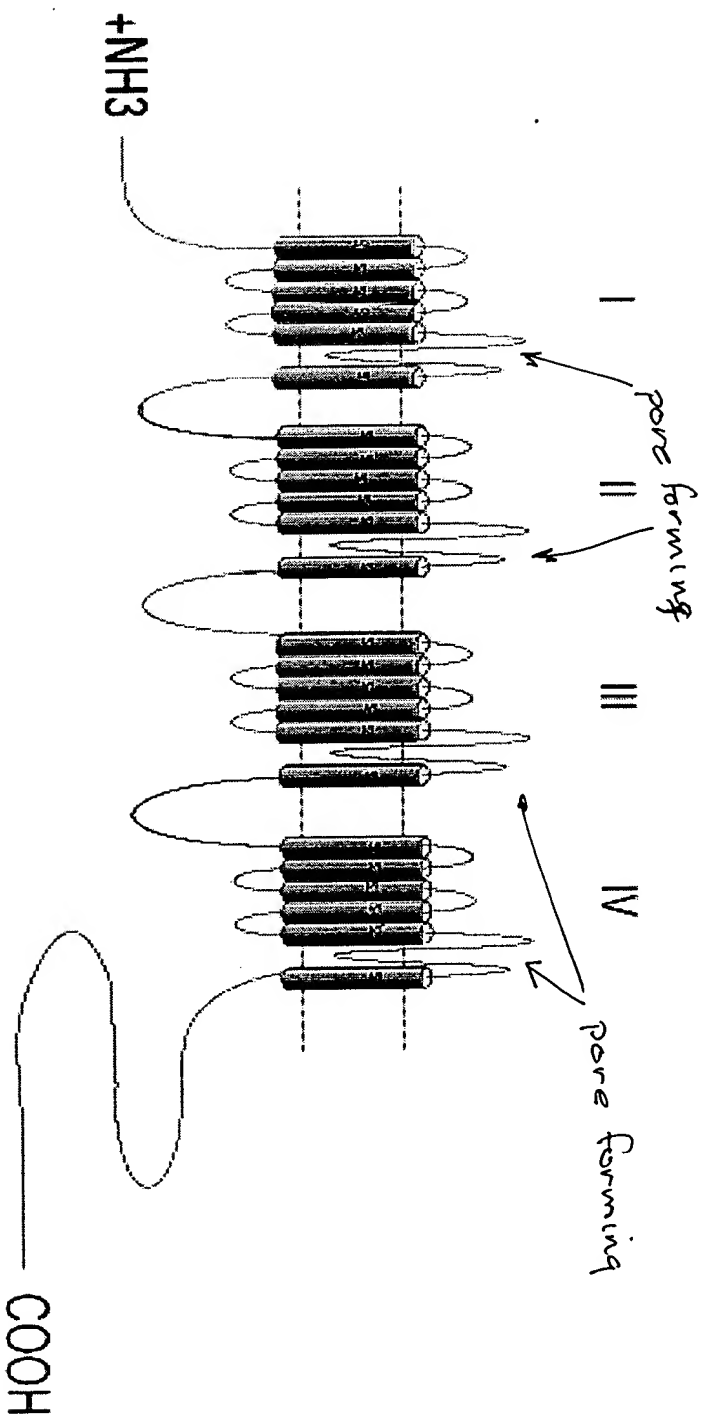


Exhibit D page 2

Molecular Diversity of the Calcium Channel $\alpha_2\delta$ Subunit

Norbert Klugbauer, Lubica Lacinová, Elsé Marais, Muriel Hobom, and Franz Hofmann

Institut für Pharmakologie und Toxikologie der Technischen Universität München, 80802 München, Germany

Sequence database searches with the $\alpha_2\delta$ subunit as probe led to the identification of two new genes encoding proteins with the essential properties of this calcium channel subunit. Primary structure comparisons revealed that the novel $\alpha_2\delta$ -2 and $\alpha_2\delta$ -3 subunits share 55.6 and 30.3% identity with the $\alpha_2\delta$ -1 subunit, respectively. The number of putative glycosylation sites and cysteine residues, hydropathicity profiles, and electrophysiological character of the $\alpha_2\delta$ -3 subunit indicates that these proteins are functional calcium channel subunits. Coexpression of $\alpha_2\delta$ -3 with α_{1C} and cardiac β_2a or α_{1E} and β_3 subunits shifted the voltage dependence of channel activation and inactivation in a hyperpolarizing direction and accelerated

the kinetics of current inactivation. The kinetics of current activation were altered only when $\alpha_2\delta$ -1 or $\alpha_2\delta$ -3 was expressed with α_{1C} . The effects of $\alpha_2\delta$ -3 on α_{1C} but not α_{1E} are indistinguishable from the effects of $\alpha_2\delta$ -1. Using Northern blot analysis, it was shown that $\alpha_2\delta$ -3 is expressed exclusively in brain, whereas $\alpha_2\delta$ -2 is found in several tissues. *In situ* hybridization of mouse brain sections showed mRNA expression of $\alpha_2\delta$ -1 and $\alpha_2\delta$ -3 in the hippocampus, cerebellum, and cortex, with $\alpha_2\delta$ -1 strongly detected in the olfactory bulb and $\alpha_2\delta$ -3 in the caudate putamen.

Key words: $\alpha_2\delta$ subunit; voltage-activated channel; calcium channel subunit; neuron; gene diversity; electrophysiology

Voltage-gated calcium channels have been purified and cloned from various tissues such as skeletal muscle, heart, and brain. These channels are formed by heterooligomeric complexes consisting of various combinations of an α_1 protein with auxiliary $\alpha_2\delta$, β , and γ subunits. To date, seven genes encoding α_1 subunits of the high voltage-activated (for review, see Hofmann et al., 1994; Strom et al., 1998; Bech-Hansen et al., 1998) and two genes of the low voltage-activated calcium channels have been identified (Perez-Reyes et al., 1998; Cribbs et al., 1998). This subunit accounts not only for the ion channel pore but also contains the voltage sensor and the determinants for binding of drugs and toxins. The current through the α_1 subunit is modulated by interactions with the β , $\alpha_2\delta$, and γ subunits. The molecular diversity of the β subunit is not only caused by the expression of four genes, but also by differential splicing. Until recently, only a single γ subunit in skeletal muscle had been described (Eberst et al., 1997), but a novel neuronal form has since been identified in brain (Letts et al., 1998).

Since the molecular cloning of the $\alpha_2\delta$ subunit (Ellis et al., 1988), several splice variants have been detected, but no further $\alpha_2\delta$ subunit genes have been identified. The different splice variants arise from various combinations of three alternatively spliced regions that result in five isoforms that are expressed in a tissue-specific manner (Angelotti and Hofmann, 1996). Structurally, the $\alpha_2\delta$ subunit is a heavily glycosylated 175 kDa protein that is posttranslationally cleaved to yield a disulfide-linked α_2 and δ protein (DeJongh et al., 1990; Jay et al., 1991). The δ part anchors the α_2 protein to the membrane via a single transmembrane

segment (Gurnett et al., 1996). The membrane topology of the $\alpha_2\delta$ subunit was further refined using anti- α_2 antibodies and C-terminal deletion mutants (Brickley et al., 1995; Wiser et al., 1996). Structural studies have shown that the extracellular α_2 domain provides the structural elements required for channel stimulation (Gurnett et al., 1996) and that the δ domain, which contains the only transmembrane segment of $\alpha_2\delta$ complex, harbors the regions important for the shift in voltage-dependent activation, steady-state inactivation, and the modulation of the inactivation kinetics (Felix et al., 1997). The identification of new $\alpha_2\delta$ subunits could present further possibilities for differential and specific regulation of calcium channels.

In studies designed to address the diversity and function of $\alpha_2\delta$, cloning, hybridization, and patch-clamp techniques were used to identify and characterize novel $\alpha_2\delta$ subunits. Two new $\alpha_2\delta$ genes were found by searching databases with the $\alpha_2\delta$ cDNA sequence (Ellis et al., 1988). These genes encode proteins with essential features of $\alpha_2\delta$ subunits, such as the high number of potential glycosylation sites and cysteine residues, the hydrophobicity plots, and electrophysiological characteristics. The novel $\alpha_2\delta$ -2 gene was found to be predominately expressed in heart, pancreas, and skeletal muscle, with $\alpha_2\delta$ -3 expressed only in brain.

MATERIALS AND METHODS

Isolation of RNA and cDNA library construction. Total RNA from mouse brain was isolated by the guanidinium thiocyanate method, and the poly(A) RNA was separated by oligo-dT cellulose chromatography (Poly(A) Quik mRNA Isolation kit; Stratagene, Heidelberg, Germany). Poly(A) RNA from mouse brain was reverse-transcribed, and double-strand cDNA was synthesized using the Superscript plasmid system (Life Technologies). The cDNA fragments were ligated with *Bst*XI/*Eco*RI adaptors (Invitrogen, San Diego, CA) and size-fractionated in a low-melting agarose gel. Only gel slices containing fragments >2000 bp were excised and digested with *Gel*ase (Biozym, Hessisch Oldendorf, Germany). Recovered cDNA was ligated into the *Bst*XI site of the pcDNAIII vector (Invitrogen) and transformed in the *Escherichia coli* XL1-blue mrf' strain (Stratagene, Heidelberg, Germany). The cDNA library was screened with a random-primed labeled PCR probe (see below, nt 1501–1821). Sequencing of the clones was performed using the dideoxy

Received Sept. 14, 1998; revised Nov. 2, 1998; accepted Nov. 3, 1998.

This work was supported by the Deutsche Forschungsgemeinschaft and Fond der Chemie.

Correspondence should be addressed to Dr. Norbert Klugbauer, Institut für Pharmakologie und Toxikologie der Technischen Universität München, Biedersteiner Strasse 29, 80802 München, Germany.

Dr. Lacinová contributed to this paper while on leave from Institute of Molecular Physiology and Genetics, Slovak Academy of Sciences, Vlárska 5, 833 04 Bratislava, Slovakia.

Copyright © 1999 Society for Neuroscience 0270-6474/99/190684-08\$05.00/0

Exhib A-F

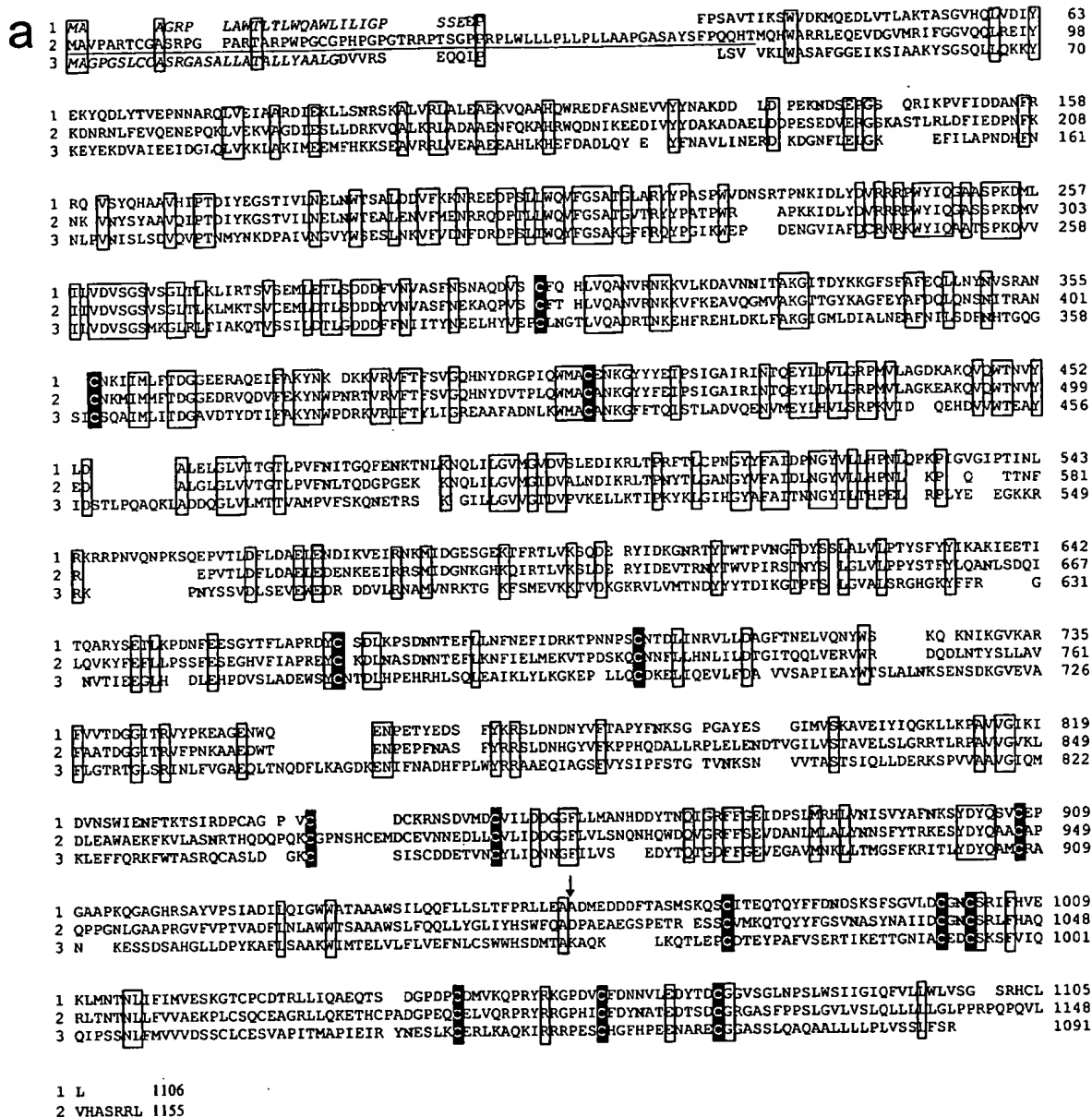


Figure 1. *a*, Amino acid alignment of the $\alpha_2\delta$ -1 (1), $\alpha_2\delta$ -2 (2), and $\alpha_2\delta$ -3 (3) subunits. The N-terminal region differing between the $\alpha_2\delta$ -2 subunit isoform I and II is underlined. Regions that are identical in all sequences are boxed, and conserved cysteine residues are additionally highlighted. The presumptive signal peptides for classes 1 and 3 are shown in italics. Potential *N*-glycosylation sites are printed in bold. The arrow indicates the cleavage site between the α_2 and δ proteins of the $\alpha_2\delta$ -1 subunit. These sequence data are available from the EMBL database under accession numbers M21948 for the $\alpha_2\delta$ -1 subunit, AF042792 for the $\alpha_2\delta$ -2(I) subunit, and AF042793 for the $\alpha_2\delta$ -2(II) subunit isoforms, respectively, and AJ010949 for the $\alpha_2\delta$ -3 subunit. *b*, Hydrophobicity profile of the $\alpha_2\delta$ subunits computed according to Kyte and Doolittle (1982). The curve is the average of a residue-specific hydrophobicity index over a window of nine residues.

chain termination method on both strands. A full-length clone was used for the preparation of the *NotI*-*SphI* fragment with the entire open reading frame in pcDNA3 (Invitrogen) yielding the expression plasmid pc3 $\alpha_2\delta$ -3.

PCR amplification. The expressed sequence tag (EST) with the accession number AA190607 was used to design the primers NKAD1, GGC ACA GAT GTC CCA GTT AAA GA and NKAD2, TGT ATA GTA GTA GTC ATT GGT CAT, with which the partial $\alpha_2\delta$ -3 subunit cDNA was amplified. The PCR fragment was cloned in pUC18 and was sequenced on both strands.

Northern blot analysis. Human and mouse multiple tissue Northern Blots were obtained from Clontech (Heidelberg, Germany) and hybridized according to the manufacturer's instructions. Random-primed labeled fragments ($\alpha_2\delta$ -2, nt 2877-3249; $\alpha_2\delta$ -3, nt 2893-3377) were used as probes; these regions share no significant homology with each other. A 3 hr prehybridization step was followed by an overnight hybridization with 5×10^6 cpm/ml of probe at 42°C. The final stringency wash performed was with $0.1 \times$ SSC, 0.1% SDS at 42°C.

In situ hybridization. Intact brains of adult female mice were removed immediately after cervical dislocation and frozen in isopentane cooled to -40°C . Brain was sectioned into 16 μm slices in a cryostat at -20°C and thaw-mounted onto polylysine slides. The tissue was vacuum-dried, fixed in 4% paraformaldehyde in PBS, and washed in $0.5 \times$ SSC. The sections were acetylated in 0.25% acetic anhydride in 0.1 M triethanolamine, pH 8.0, and washed in $2 \times$ SSC. The tissue was dehydrated through a series of ethanol solutions, from 50 to 100%. The slides were vacuum-dried and stored at -80°C until used.

Murine $\alpha_2\delta$ -1 (nt 2760-3170), human $\alpha_2\delta$ -2 (nt 2877-3249), and murine $\alpha_2\delta$ -3 (nt 2744-3228) specific riboprobes were generated by *in vitro* transcription as described previously (Ludwig et al., 1997). Briefly, probe template DNA was amplified by PCR from murine $\alpha_2\delta$ -1 and -2 clones using primers specific for the variable C-terminal region of α_2 . *Bam*HI and *Asp*718 restriction sites were added to the $\alpha_2\delta$ -1 forward and reverse primers, respectively, to allow for sticky-end ligation. $\alpha_2\delta$ -3 was ligated to the linearized vector by blunt end ligation. The integrity of each probe was verified by dideoxy termination sequencing. ^{35}S -UTP (DuPont NEN, Wilmington, DE)-labeled sense and antisense riboprobes were generated using a standard T3 and T7 polymerase *in vitro* transcription procedure (T3 and T7 from New England Biolabs, Beverly, MA). Unincorporated nucleotides were removed using Sephadex G50 columns (Pharmacia, Freiburg, Germany).

Messenger RNA *in situ* hybridization was performed on cryostat sections of mouse brain. A prehybridization step was performed at 45°C for 2 hr. Hybridization with 1×10^7 cpm/ml probe proceeded for 16 hr at 55°C . After a 20 $\mu\text{g}/\text{ml}$ RNase A (Boehringer Mannheim, Mannheim, Germany) digestion, a high-stringency wash of $0.1 \times$ SSC, 1 mM EDTA, and 1 mM dithiothreitol was done for 2 hr at 60°C . The slides were dehydrated in ethanol and analyzed by autoradiography.

Transfection of HEK293 cells and electrophysiological recordings. The full-length cDNAs of all subunits, i.e., α_{1C} , α_{1E} , $\beta_2\alpha$, β_3 , $\alpha_2\delta$ -1, and $\alpha_2\delta$ -3 were cloned into the pcDNA 3 vector (Invitrogen). For more details, see Schuster et al. (1996). HEK 293 cells were transfected with various combinations of an α_1 subunit (α_{1C} , α_{1E}), a β subunit ($\beta_2\alpha$, β_3), and an $\alpha_2\delta$ subunit ($\alpha_2\delta$ -1, $\alpha_2\delta$ -3). This was achieved by lipofection with Lipofectamine (Life Technologies) at a DNA mass ratio of 1:1 for expression of two subunits or 1:1:1 for three subunits.

Electrophysiological recordings. Ionic currents from transfected cells were recorded in whole-cell configuration of the patch-clamp method. Ba^{2+} was used as the charge carrier. The extracellular solution contained (in mM): *N*-methyl-D-glucamine, 125; BaCl_2 , 20; CsCl , 5; MgCl_2 , 1; HEPES, 10; and glucose, 5, pH 7.4 (HCl). The intracellular solution contained (in mM): CsCl , 60; CaCl_2 , 1; EGTA, 11; MgCl_2 , 1; K_2ATP , 5; HEPES, 10; and aspartic acid, 50, pH 7.4 (CsOH). Currents were recorded using an EPC-9 patch-clamp amplifier and corresponding Pulse software from Heka Electronics (Lambrecht, Germany). Patch pipettes were pulled from borosilicate glass. The pipette input resistance was typically between 1.8 and 2.2 M Ω . The capacity of individual cells ranged between 25 and 90 pF, and series resistance ranged between 3.5 and 5.0 M Ω . Capacity transients were compensated using build-in procedure of the Heka system. Curve fitting and statistical analysis were performed using the Origin 5.0 software package (Microcal, Northampton, MA). The significance of observed differences was evaluated by nonpaired Student's *t* test. Probability of 5% or less was considered to be significant.

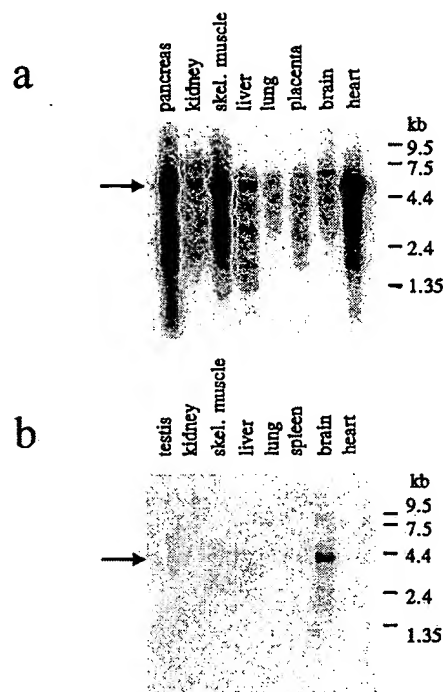


Figure 2. Northern blot analysis of the $\alpha_2\delta$ -2 and $\alpha_2\delta$ -3 subunits. For each lane, $\sim 2 \mu\text{g}$ of poly(A) RNA was run on a denaturing formaldehyde-containing agarose gel, transferred to a nylon membrane, and fixed by UV irradiation. *a*, Human multiple tissue blot using a specific probe for the $\alpha_2\delta$ -2 subunit. *b*, Mouse multiple tissue blot for the $\alpha_2\delta$ -3 subunit. Arrows indicate predominant species of mRNA with sizes of 5.2 ($\alpha_2\delta$ -2) and 4.3 ($\alpha_2\delta$ -3) kb.

RESULTS

Primary structures

A database search using the $\alpha_2\delta$ subunit cDNA as probe revealed three additional sequences similar to this calcium channel subunit (Fig. 1), which were derived from two genes named 2 and 3. Two of these sequences are human full-length sequences of closely related isoforms of the $\alpha_2\delta$ subunit (GenBank accession numbers: AF042792, isoform I; AF042793, isoform II; M. H. Wei, F. Latif, F. M. Duh, D. Andreazzoli-Angeloni, V. Kashuba, E. Zabarovsky, B. Johnson, and M. I. Lerman, unpublished observations). These sequences differ only at the N terminus of the α_2 protein, indicating that both isoforms are derived from the same gene 2 and are generated by differential splicing. The 5'-untranslated region upstream of the ATG codon from isoform I is in good agreement with the Kozak sequence for initiation of translation in eukaryotic cells, whereas the same region of isoform II shows only a limited homology with this sequence. Furthermore, only isoform I but not isoform II shows features of a potential signal sequence. Both observations suggest that only isoform I can form a functional calcium channel subunit. Isoform I, which we describe here as the $\alpha_2\delta$ -2 subunit, (Wei, Latif, Duh, Andreazzoli-Angeloni, Kashuba, Zabarovsky, Johnson, and Lerman, unpublished observations) has 55.6% identity with the $\alpha_2\delta$ -1 subunit (Ellis et al., 1988). Eighteen potential *N*-glycosylation sites can be identified in the primary structure (Fig. 1), which is the same number of sites as in the $\alpha_2\delta$ -1 subunit (Ellis et al., 1988).

The third sequence identified by database searches was a partial human EST sequence AC: AA190607. This sequence was

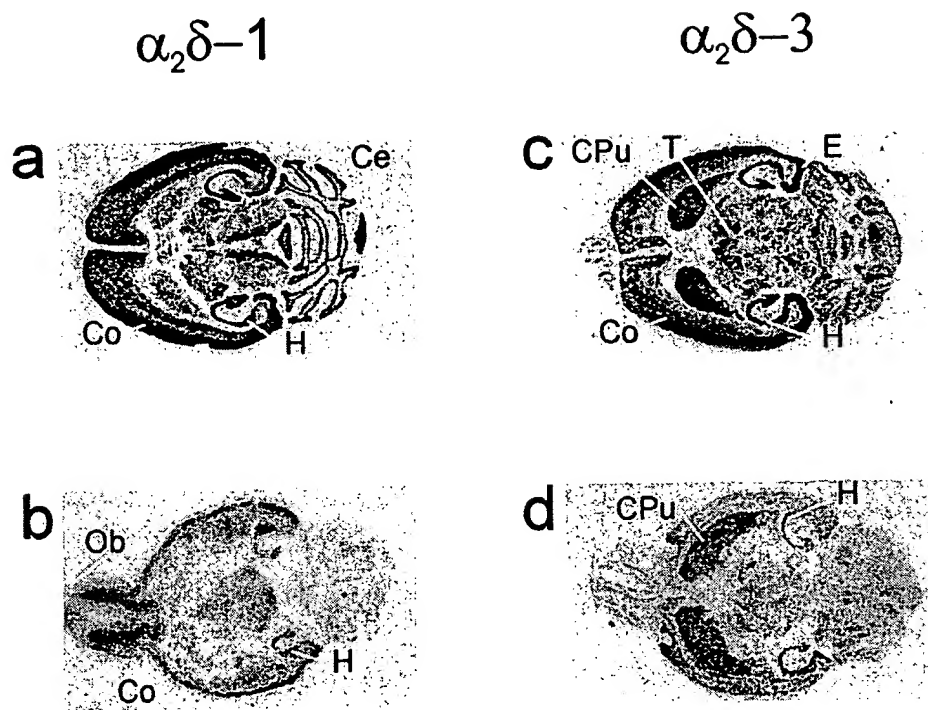


Figure 3. Autoradiographs of $\alpha_2\delta$ -1 and $\alpha_2\delta$ -3 riboprobe hybridization to horizontal mouse brain sections. Central (*a*, *c*) and more basal (*b*, *d*) sections of the brain are shown. Expression of $\alpha_2\delta$ -1 is seen in the (*a*) hippocampus (*H*), cerebral cortex (*Co*), cerebellum (*Ce*), and (*b*) olfactory bulb (*Ob*). $\alpha_2\delta$ -3 mRNA was detected in the caudate putamen (*CPu*), hippocampus (*H*), entorhinal complex (*E*), cortex (*Co*), and thalamic nuclei (*T*) (*c*, *d*).

used to design primers for the amplification of cDNA from mouse tissues. The cDNA could be amplified only from mouse brain mRNA and not from other tissues (Fig. 2). A cDNA library was constructed from mouse brain mRNA and screened with the PCR product as a probe. Several independent clones could be identified that encode the novel $\alpha_2\delta$ subunit, which we name $\alpha_2\delta$ -3 (Fig. 1). A detailed restriction analysis of the different clones showed that there are no further isoforms in mouse brain. The sequence upstream of the start ATG is in agreement with that for the initiation of translation in eukaryotic cells (data not shown). The open reading frame consists of 3273 bp encoding a protein with 1091 amino acid residues. The $\alpha_2\delta$ -3 subunit has 30.3% identity with the $\alpha_2\delta$ -1 subunit and 31.2% with the $\alpha_2\delta$ -2 subunit. The primary structure of $\alpha_2\delta$ -3 contains nine potential *N*-glycosylation sites (Fig. 1*a*).

Hydrophobicity analysis of all three $\alpha_2\delta$ subunits indicates a similar membrane topology, including a hydrophobic transmembrane segment at the C terminus of the δ domain (Fig. 1*b*). A sequence comparison reveals that as many as 14 cysteine residues are conserved in all of the three $\alpha_2\delta$ genes, further strengthening the postulate that these subunits are disulfide-linked proteins with similar higher order structures.

Tissue distribution

The expression of the novel $\alpha_2\delta$ subunits was examined by Northern and *in situ* hybridization. The $\alpha_2\delta$ -2 subunit is highly expressed in heart, pancreas, and skeletal muscle tissue (Fig. 2), which can be seen even after 6 hr of autoradiography of Northern blots. After 1 d of exposure, the $\alpha_2\delta$ -2 subunit can also be detected in kidney, liver, placenta, and brain. This broad expression pattern was also observed for the $\alpha_2\delta$ -1 subunit. An 8.0 kb transcript of the $\alpha_2\delta$ -1 subunit was detected in brain, heart, aorta, skeletal muscle, and ileum (Ellis et al., 1988). In contrast to this ubiquitous expression pattern, the $\alpha_2\delta$ -3 subunit is only found in brain (Fig. 2). In each case, the Northern analysis reveals one

predominant species of mRNA with sizes of 5.2 (class 2) and 4.3 kb (class 3).

The mRNA expression of $\alpha_2\delta$ -1 and $\alpha_2\delta$ -3 calcium channel subunits in mouse brain was mapped by *in situ* hybridization. Both $\alpha_2\delta$ forms were detected in several regions of the brain, with differential expression of the mRNAs in some structures. Strong expression of $\alpha_2\delta$ -1 was seen in the pyramidal cell layer of Ammon's horn in the hippocampus (CA1–3) and in the granular cell layer of the dentate gyrus (Fig. 3). The olfactory bulb also stained strongly, and expression in the mitral and glomerular cell regions was seen by dark-field microscopy of slides coated with photographic emulsion. Signals in the cerebellar cortex, and to a lesser extent in thalamic nuclei, were also observed (Fig. 3). Examination of emulsion-coated slides showed that the expression of $\alpha_2\delta$ -1 in the cerebellum was restricted to the granular layer (data not shown).

The $\alpha_2\delta$ -3 mRNA was predominantly expressed in the caudate putamen, entorhinal complex, hippocampus, and cortex (Fig. 3). As with $\alpha_2\delta$ -1, the pyramidal cell layer of the hippocampus (CA1–3) and granular cell layer of the dentate gyrus showed the highest degree of hybridization with the antisense probe (Fig. 3). Hybridization of both probes was specific as judged by the absence of signals when sense probes were applied (data not shown). *In situ* hybridization for the $\alpha_2\delta$ -2 subunit indicated a ubiquitous expression in cardiac tissues (data not shown).

Functional characterization

Because the Northern blot hybridization indicated a high expression of the $\alpha_2\delta$ -3 subunit in brain, we performed cotransfection studies with α_1 subunits that have been characterized in this tissue. Because *in situ* analysis did not show an exact colocalization of $\alpha_2\delta$ -3 with known α_1 subunits, coexpression studies were done with an α_1 subunit of the dihydropyridine-sensitive class C

and a dihydropyridine-insensitive class E calcium channel. This approach allows for the identification of interactions with both evolutionary distant calcium channel α_1 families.

Effects of the $\alpha_2\delta$ -3 subunit on barium current through the α_{1C} -type calcium channel

To study the effects of $\alpha_2\delta$ -3 subunit on channel gating, we coexpressed this subunit with the α_{1C} subunit alone or in combination with both α_{1C} and β_2a subunits. Voltage protocols are described in detail in the legend to Figure 4, and quantitative analyses are summarized in Table 1. When coexpressed with α_{1C} alone, the effects of $\alpha_2\delta$ -3 on I_{Ba} were less noticeable than when β_2a was coexpressed. $\alpha_2\delta$ -3 did not affect the current density, time course of current inactivation, and voltage dependence of steady-state inactivation of α_{1C} expressed singly (data not shown). However, when expressed with α_{1C} only, $\alpha_2\delta$ -3 shifted the activation curve by 4.4 mV in the hyperpolarizing direction and slightly accelerated the time of current activation during the depolarizing pulse (data not shown). The effects on the channel kinetics became more prominent in the presence of the β_2a subunit (Fig. 4, Table 1). In this combination, $\alpha_2\delta$ -3 significantly increased the current density, shifted the voltage dependence of current activation by 8.7 mV in a hyperpolarizing direction, accelerated the time course of current activation during the depolarizing pulse, accelerated the current inactivation at positive membrane potentials, shifted the steady-state inactivation curve in a hyperpolarizing direction, and significantly changed its slope.

We further compared the effects of $\alpha_2\delta$ -3 with those of the previously described $\alpha_2\delta$ -1 subunit (Fig. 4, Table 1). The changes in gating-related channel characteristics elicited by both subunits were qualitatively similar, and in most cases the measurements (current density, voltage dependence of current activation and inactivation, and time course of current activation) were not significantly different. Both $\alpha_2\delta$ -1 and -3 subunits accelerated the time course of current inactivation at a membrane potential of +20 mV by enhancing the proportion of the fast time constant, τ_1 . $\alpha_2\delta$ -3 changed this constant from 273 ± 24 msec to 156 ± 10 msec. Surprisingly, $\alpha_2\delta$ -1 significantly increased the value of the slow time constant τ_2 from 1.16 ± 0.08 sec to 3.54 ± 0.46 sec, but this effect was apparently overwhelmed by the effect of the increased proportion of the current inactivating with fast time constant τ_1 , with the result that the overall time course of inactivation was accelerated (Fig. 4*b*, inset). The effects of both $\alpha_2\delta$ -3 and $\alpha_2\delta$ -1 subunits on whole-cell current parameters, which reflect the gating of the α_{1C} channel, are virtually identical and they require the presence of β (in this case β_2a) to become prominent.

Effects of the $\alpha_2\delta$ -3 subunit on barium current through α_{1E} -type calcium channel

Although both α_{1C} and $\alpha_2\delta$ -1 subunits are fairly abundant in mammalian tissues, α_{1E} and $\alpha_2\delta$ -3 are predominantly expressed in neuronal tissue. We therefore selected α_{1E} for studying the effects of $\alpha_2\delta$ -3. For all experiments, β_3 subunit was coexpressed with α_{1E} . This β subunit was suggested to modulate the current through the α_{1E} channel (Ludwig et al., 1997). As with the α_{1C} channel, both $\alpha_2\delta$ -1 and $\alpha_2\delta$ -3 affected most of the gating-related parameters except for the time constant of current activation during membrane depolarization (Fig. 5, Table 1). In contrast to $\alpha_{1C}\beta_2a$ channel, the effects of $\alpha_2\delta$ -3 and $\alpha_2\delta$ -1 on the voltage dependence of current activation (Fig. 5*a*) and inactivation (Fig. 5*b*) of $\alpha_{1E}\beta_3$ channel were significantly different. The $\alpha_2\delta$ -1

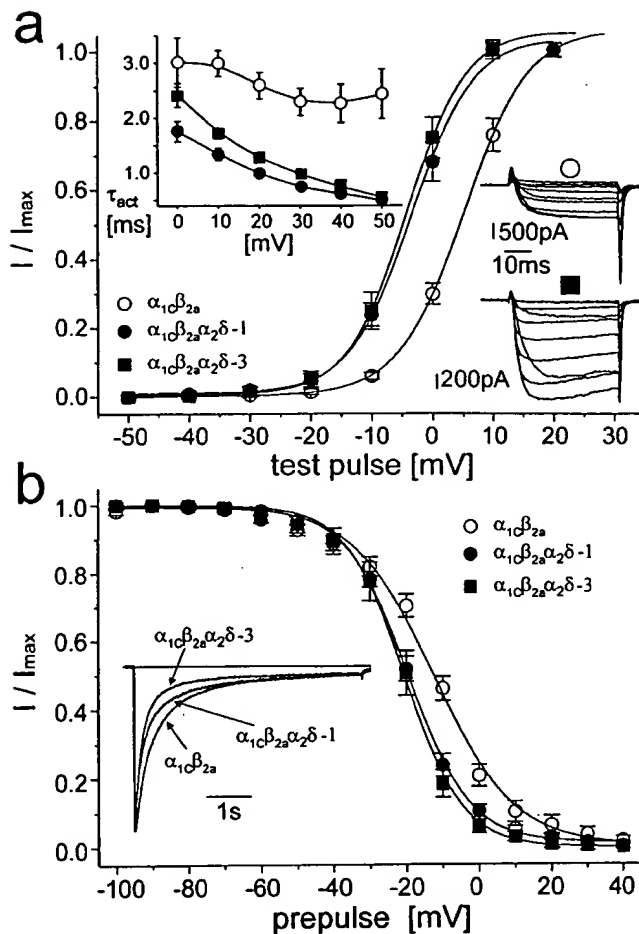


Figure 4. The $\alpha_2\delta$ subunit affects current through the α_{1C} -type calcium channel. The $\alpha_2\delta$ -3 subunit was coexpressed with α_{1C} and β_2a . For comparison, the current through cells coexpressing $\alpha_2\delta$ -1 subunit was coanalyzed. *a* shows the voltage dependence of current activation measured as the amplitude of current activated by a 40-msec-long depolarizing pulse from a holding potential of -80 mV to voltages marked on the ordinate and normalized to the maximal amplitude. Each voltage dependence was fitted to the Boltzmann equation. Results of these fits are summarized in Table 1. The inset in the top left of *a* shows voltage dependence of the kinetics of current activation. The ascending phase of the current time course was fitted to single exponential. The resulting time constants were averaged and plotted against corresponding membrane potentials. In both graphs, \circ represents the $\alpha_{1C}\beta_2a$ channel, \bullet the $\alpha_{1C}\beta_2a\alpha_2\delta$ -1 channel, and \blacksquare the $\alpha_{1C}\beta_2a\alpha_2\delta$ -3 channel. The inset in the right of *a* illustrates a typical family of currents measured during a series of depolarizing pulses from the holding potential of -80 mV to membrane potentials ranging from -20 to $+70$ mV with a step of $+10$ mV. \circ , $\alpha_{1C}\beta_2a$ channel. The cell capacity was 83 pF, and the resulting maximal current density was approximately -13 pA/pF; \blacksquare , $\alpha_{1C}\beta_2a\alpha_2\delta$ -3. The cell capacity was 31 pF, and the corresponding maximal current density was approximately -41 pA/pF. *b* shows averaged steady-state inactivation curves measured from a holding potential of -80 mV. Current was inactivated by a 5-sec-long prepulse to the potentials marked on the ordinate. This was followed by a 5-msec-long return to the holding potential and a 40-msec-long test pulse to the maximum of the current-voltage relationship. Solid lines are fitted to the Boltzmann equation. The inset shows the time course of the current during a 5-sec-long depolarizing pulse to $+20$ mV with zero level indicated by a horizontal line. Currents shown are averaged time courses from 9 to 12 experiments scaled to the same amplitude. Individual measurements were fitted to the sum of two exponentials. Results of all fitting procedures are summarized in Table 1. Symbols are as in *a*.

Table 1. Comparison of the effects of $\alpha_2\delta$ -1 and $\alpha_2\delta$ -3 subunits on I_{Ba} through α_{1C} or α_{1E} -type calcium channels

| | $\alpha_{1C}\beta 2a$ | $\alpha_{1C}\beta 2a\alpha_2\delta$ -1 | $\alpha_{1C}\beta 2a\alpha_2\delta$ -3 | $\alpha_{1E}\beta 3$ | $\alpha_{1E}\beta 3\alpha_2\delta$ -1 | $\alpha_{1E}\beta 3\alpha_2\delta$ -3 |
|-------------------------------|-----------------------|--|--|----------------------|---------------------------------------|---------------------------------------|
| I_{Ba} density (pA/pF) | 13.8 ± 1.4 (16) | 30.3 ± 6.6* (15) | 28.6 ± 4.9* (21) | 24.4 ± 5.4 (12) | 98.1 ± 20.0*** (10) | 95.4 ± 15.6*** (10) |
| $V_{0.5 \text{ activ.}}$ (mV) | +5.2 ± 0.1 (16) | -5.0 ± 0.6*** (13) | -3.5 ± 0.5*** (11) | -13.0 ± 1.1 (10) | -14.5 ± 0.2 (9) | -20.1 ± 0.7***, ^{aaa} (11) |
| $k_{\text{activ.}}$ | 5.4 ± 0.1 | 5.1 ± 0.4 | 5.1 ± 0.4 | 5.6 ± 0.9 | 3.7 ± 0.1 | 4.6 ± 0.6 |
| $V_{0.5 \text{ inact.}}$ (mV) | -12.5 ± 0.9 (9) | -19.6 ± .3*** (14) | -20.5 ± 0.4*** (8) | -64.4 ± 0.4 (9) | -69.7 ± 0.4*** (11) | -76.2 ± 0.5***, ^{aaa} (9) |
| $k_{\text{inact.}}$ | 11.1 ± 0.7 | 8.5 ± 0.2*** | 8.0 ± 0.3** | 7.1 ± 0.4 | 8.4 ± 0.4* | 9.5 ± 0.4*** |
| A1 (%) | 61.1 ± 3.9 (12) | 73.7 ± 4.5* (11) | 78.1 ± 2.6** (9) | 93.0 ± 2.1 (8) | 97.3 ± 0.5* (10) | 98.5 ± 0.5** (10) |
| τ_1 (msec) | 273 ± 24 | 260 ± 19 | 156 ± 10***, ^{aaa} | 31.9 ± 5.7 | 23.6 ± 0.9 | 24.1 ± 1.7 |
| τ_2 (sec) | 1.16 ± 0.08 | 3.54 ± 0.46*** | 0.90 ± 0.10 ^{aaa} | | | |

The data are the means ± SEM. The number of experiments performed is indicated in parentheses. The first row compares the average current density for each channel. The second row compares voltage dependence of current activation of different subunit combinations. The ascending part of the I - V curve, which is shown in panel *a* of Figures 4 and 5 was fitted to the Boltzmann function. $V_{0.5 \text{ activ.}}$ and $k_{\text{activ.}}$ are the parameters of these fits. The fourth row compares voltage dependence of current inactivation. The steady-state inactivation curves shown in panel *b* of Figures 4 and 5 were fitted to the Boltzmann function. $V_{0.5 \text{ inact.}}$ and $k_{\text{inact.}}$ are parameters of Boltzmann fits. The last three rows show the results of fitting the time course of inactivation of I_{Ba} during a 5-sec-long (α_{1C} -derived channels, traces shown in Figure 4*b*) or 300-msec-long (α_{1E} -derived channels, traces shown in Figure 5*b*) depolarizing pulse to +20 mV. Currents through α_{1C} -derived channels were fitted to a sum of two exponentials. A1 represents the relative amplitude of the current inactivating with the fast time constant τ_1 . α_{1E} -derived channels were found to inactivate with single time constant. For these channels, 100-A1 represents the relative amplitude of the noninactivating component of the current remaining at the end of the depolarizing pulse (see also Fig. 5*b*). The significance of the difference was tested using the unpaired Student's *t* test. Asterisks (*) indicate the statistical significance between $\alpha_{1C}\beta 2a$ and $\alpha_{1C}\beta 2a\alpha_2\delta$ -1 or $\alpha_{1C}\beta 2a\alpha_2\delta$ -3 and between $\alpha_{1E}\beta 3$ and $\alpha_{1E}\beta 3\alpha_2\delta$ -1 or $\alpha_{1E}\beta 3\alpha_2\delta$ -3. Significant difference between $\alpha_{1C}\beta 2a\alpha_2\delta$ -1 and $\alpha_{1C}\beta 2a\alpha_2\delta$ -3 and between $\alpha_{1E}\beta 3\alpha_2\delta$ -1 and $\alpha_{1E}\beta 3\alpha_2\delta$ -3 is marked by (*).

* $p < 0.05$; ** $p < 0.01$; *** $p < 0.001$; ^{aaa} $p < 0.001$.

subunit shifted both activation and steady-state inactivation curves in a hyperpolarizing direction, but the change in current activation was not statistically significant. In both curves, the shift evoked by $\alpha_2\delta$ -3 was significantly larger (Table 1). In contrast, the effects of both $\alpha_2\delta$ s on the time course of current inactivation at a membrane potential of +20 mV were identical and restricted to diminution of the noninactivating part of the current (Table 1).

DISCUSSION

We present here the first account of the existence of multiple $\alpha_2\delta$ calcium channel subunits. The previously known $\alpha_2\delta$ we have named $\alpha_2\delta$ -1, and the new forms have been designated $\alpha_2\delta$ -2 and $\alpha_2\delta$ -3 based on their similarity to the original subunit. An amino acid alignment reveals that there is only a significant degree of homology in the core region of the α_2 protein, whereas the δ proteins show identities only with respect to the cysteine residues. Despite the low degree of homology at the primary structure level between these forms, other features such as the number of glycosylation sites, cysteine residues, and hydrophobicity profiles are very similar. For these reasons we conclude that all three $\alpha_2\delta$ subunits are disulfide-linked proteins with similar higher order structures. The $\alpha_2\delta$ -1 and -2 subunits are more ubiquitously expressed than $\alpha_2\delta$ -3, which has only been identified in brain. Comparisons of the expression patterns of the 1 and 3 class $\alpha_2\delta$ subunits with α_1 subunits in brain slices (Ludwig et al., 1997) do not indicate specific α_1 - $\alpha_2\delta$ combinations. We cannot exclude the possibility that $\alpha_2\delta$ -3 also interacts with other ion channels or even other membrane proteins.

Functional coexpression of the $\alpha_2\delta$ -1 subunit with various combinations of α_1 and β subunits results in an increase in the current densities or dihydropyridine (DHP)-binding sites (Singer et al., 1991; Welling et al., 1993; De Waard et al., 1995; Shistik et al., 1995; Bangalore et al., 1996; Gurnett et al., 1996; Felix et al., 1997; Parent et al., 1997; Jones et al., 1998), acceleration of current activation and inactivation (Singer et al., 1991; De Waard et al., 1995; Bangalore et al., 1996; Felix et al., 1997; Qin et al., 1998; Shirokov et al., 1998), and a shift of the current-voltage curve in a hyperpolarizing direction (Singer et al., 1991; Felix et al., 1997). Regardless of the α_1 subunit used in this study, the $\alpha_2\delta$ -3 subunit

was found to increase the current density, which is in agreement with the results of these groups. In addition to this effect, coexpression of $\alpha_2\delta$ -3 caused a shift of the voltage dependence of channel activation and inactivation in a hyperpolarizing direction and an acceleration in the kinetics of current inactivation.

When the results shown in Figures 4 and 5 are compared, it can be seen that $\alpha_2\delta$ -1 caused a smaller shift in the voltage dependence of activation and inactivation of $\alpha_{1E}\beta 3$ as compared with the $\alpha_{1C}\beta 2a$ channel. The effects of $\alpha_2\delta$ -3 on the electrophysiological properties of α_{1C} coexpressed with $\beta 2a$ was found to be similar to those of $\alpha_2\delta$ -1. In contrast, coexpression of $\alpha_2\delta$ -3 with α_{1E} and $\beta 3$ produced more pronounced differences in the current characteristics associated with channel gating than the coexpression of $\alpha_2\delta$ -1.

The mechanism whereby $\alpha_2\delta$ modulates the conductances of α_1 is not clearly understood. The increase in density of current and DHP-binding sites can be explained by an improved targeting of expressed α_1 subunit to the cell membrane and maturation of the channel complex (Shistik et al., 1995), which leads to an increased amount of charge moved during channel activation (Bangalore et al., 1996; Qin et al., 1998). It was suggested that the increase in current requires the presence of an intact α_2 protein, whereas the shift of voltage-dependent activation and steady state inactivation as well as the acceleration of the inactivation kinetics are caused by the transmembrane δ protein (Felix et al., 1997). However, based on the amino acid similarity of the three subunit forms, it seems more likely that α_2 harbors the relevant residues responsible for the observed effects on α_1 and that the δ domain functions only as an membrane anchor for α_2 . This interpretation is further strengthened by the sequences of the δ proteins, which are not conserved.

These results, together with the brain-specific expression of $\alpha_2\delta$ -3, suggest that the $\alpha_2\delta$ -3 subunit may have a distinct physiological role in neuronal tissue. The $\alpha_2\delta$ protein has been implicated as the *in vivo* target for the antiepileptic drug gabapentin (Gee et al., 1996), which apparently inhibits calcium currents in isolated rat brain neurons (Stefani et al., 1998). It was proposed that gabapentin binds preferentially to the $\alpha_2\delta$ -1 subunit. This is supported by evidence that the partial N-terminal amino acid

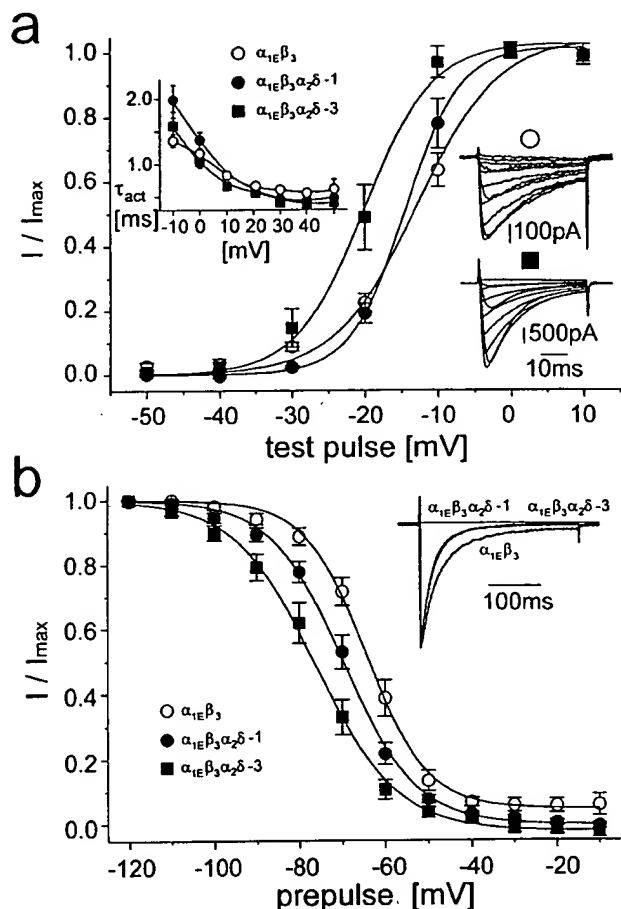


Figure 5. The $\alpha_2\delta$ subunit affects current through the α_{1E} -type calcium channel. Unless otherwise indicated, the voltage protocols used were the same as those described in the legend to Figure 4. \circ represents the $\alpha_{1E}\beta_3$ channel; \bullet the $\alpha_{1E}\beta_3\alpha_2\delta-1$ channel, and \blacksquare the $\alpha_{1E}\beta_3\alpha_2\delta-3$ channel. Boltzmann fits of voltage dependencies of current activation are summarized in Table 1. The inset in the right of *a* shows a typical family of currents measured during a series of depolarizing pulses from a holding potential of -100 mV to membrane potentials ranging from -30 mV to +60 mV with step of +10 mV. \circ , $\alpha_{1E}\beta_3$ channel, with a cell capacity of 19 pF and a maximal current density of approximately -34 pA/pF; \blacksquare , $\alpha_{1E}\beta_3\alpha_2\delta-3$ channel, with a capacity of 43 pF and a maximal current density of approximately -74 pA/pF. *b* shows the steady-state inactivation curve measured from a holding potential of -100 mV using a 5-sec-long conditioning pulse to membrane potentials marked on the ordinate. Solid lines represent Boltzmann fits. The inset illustrates the inactivation of I_{Ba} during a 300-msec-long depolarizing pulse from a holding potential of -100 mV to +20 mV scaled to the same amplitude. Eight to 10 measurements were averaged for each channel type. The $\alpha_{1E}\beta_3\alpha_2\delta-1$ and $\alpha_{1E}\beta_3\alpha_2\delta-3$ current traces are indistinguishable from each other. Individual time courses of current inactivation were fitted to a single exponential with a small proportion of noninactivating current. Results of all fits are summarized in Table 1. Symbols are as in *a*.

sequence of the gabapentin-binding protein obtained from porcine brain membranes is identical with an aminoterminal peptide of $\alpha_2\delta-1$. This sequence is not present in classes 2 or 3. Further support for this postulate is that our mRNA *in situ* analysis of $\alpha_2\delta-1$ in brain showed the same distribution as that of gabapentin-binding sites (Taylor et al., 1998), which differs from that of $\alpha_2\delta-3$. For these reasons it is more likely that gabapentin targets the $\alpha_2\delta-1$ subunit. However, another study using a different purification procedure showed that there may be an additional

gabapentin-binding protein in brain, which was detected with a polyclonal α_2 antibody (Brown et al., 1998) and which could be another $\alpha_2\delta$ form. Further investigations need to be undertaken to elucidate the binding of gabapentin to the $\alpha_2\delta$ subunit.

REFERENCES

- Angelotti T, Hofmann F (1996) Tissue-specific expression of splice variants of the mouse voltage-gated calcium channel $\alpha_2\delta$ subunit. *FEBS Lett* 397:331-337.
- Bangalore R, Mehrke G, Gingrich K, Hofmann F, Kass RS (1996) Influence of L-type Ca channel $\alpha_2\delta$ -subunit on ionic and gating current in transiently transfected HEK 293 cells. *Am J Physiol* 270:H1521-H1528.
- Beck-Hansen NT, Naylor MJ, Maybaum TA, Pearce WG, Koop B, Fishman GA, McIs M, Musarella MA, Boycott KM (1998) Loss-of-function mutations in a calcium-channel α_1 -subunit in Xp11.23 cause incomplete X-linked congenital stationary night blindness. *Nat Genet* 19:264-267.
- Brickley K, Campbell V, Berrow N, Leach R, Norman RI, Wray D, Dolphin AC, Baldwin SA (1995) Use of site-directed antibodies to probe the topography of the α_2 subunit of voltage-gated Ca^{2+} channels. *FEBS Lett* 364:129-133.
- Brown JP, Dissanayake VUK, Briggs AR, Milic MR, Gee N (1998) Isolation of the [3H] gabapentin-binding protein/ $\alpha_2\delta$ Ca^{2+} channel subunit from porcine brain: development of a radioligand binding assay for $\alpha_2\delta$ subunits using [3H]leucine. *Anal Biochem* 255:236-243.
- Cribbs LL, Lee J-H, Yang J, Satin J, Zhang Y, Daud A, Barclay J, Williamson MP, Fox M, Rees M, Perez-Reyes E (1998) Cloning and characterization of α_1H from human heart, a member of the T-type Ca^{2+} channel gene family. *Circ Res* 83:103-109.
- De Jongh KS, Warner C, Catterall WA (1990) Subunits of purified calcium channels. *J Biol Chem* 265:14738-14741.
- De Waard M, Campbell KP (1995) Subunit regulation of the neuronal α_{1A} Ca^{2+} channel expressed in *Xenopus* oocytes. *J Physiol (Lond)* 485:619-634.
- Eberst R, Dai S, Klugbauer S, Hofmann F (1997) Identification and functional characterization of a calcium channel gamma subunit. *Pflügers Arch* 433:633-637.
- Ellis SB, Williams ME, Ways NR, Brenner R, Sharp AH, Leung AT, Campbell KP, McKenna E, Koch WJ, Hui A, Schwartz A, Harpold MM (1988) Sequence and expression of mRNAs encoding the α_1 and α_2 subunits of a DHP sensitive calcium channel. *Science* 241:1661-1664.
- Felix R, Gurnett CA, De Waard M, Campbell KP (1997) Dissection of functional domains of the voltage-dependent Ca^{2+} channel $\alpha_2\delta$ subunit. *J Neurosci* 17:6884-6891.
- Gee NS, Brown JP, Dissanayake VUK, Offord J, Thurlow R, Woodruff GN (1996) The novel anticonvulsant drug, gabapentin (neurontin), binds to the $\alpha_2\delta$ subunit of a calcium channel. *J Biol Chem* 271:5768-5776.
- Gurnett CA, De Waard M, Campbell KP (1996) Dual function of the voltage-dependent Ca^{2+} $\alpha_2\delta$ subunit in current stimulation and subunit interaction. *Neuron* 16:431-440.
- Hofmann F, Biel M, Flockerzi V (1994) Molecular basis for Ca^{2+} channel diversity. *Annu Rev Neurosci* 17:399-418.
- Jay SD, Sharp AH, Kahl SD, Vedvick TS, Harpold MM, Campbell KP (1991) Structural characterization of the dihydropyridine-sensitive calcium channel α_2 -subunit and the associated δ peptides. *J Biol Chem* 266:3287-3293.
- Jones LP, Wei S-K, Yue DT (1998) Mechanisms of auxiliary subunit modulation of neuronal α_{1E} calcium channels. *J Gen Physiol* 112:125-143.
- Kyte J, Doolittle RF (1982) A simple method for displaying the hydrophobic character of a protein. *J Mol Biol* 157:105-132.
- Letts VA, Felix R, Biddlecome GH, Arikath J, Mahaffey CL, Valenzuela A, Bartlett FS, Mori Y, Campbell KP, Frankel WN (1998) The mouse stargazer gene encodes a neuronal Ca^{2+} -channel γ subunit. *Nat Genet* 19:340-347.
- Ludwig A, Flockerzi V, Hofmann F (1997) Regional expression and cellular localization of the α_1 and β subunit of high voltage-activated calcium channels in rat brain. *J Neurosci* 17:1339-1349.
- Parent L, Schneider T, Moore CP, Talwar D (1997) Subunit regulation of the human brain α_{1E} calcium channel. *J Membr Biol* 160:127-140.
- Perez-Reyes E, Cribbs LL, Daud A, Lacerda AE, Barclay J, Williamson MP, Fox M, Rees M, Lee J-H (1998) Molecular characterization of a

- neuronal low-voltage-activated T-type calcium channel. *Nature* 391:896–899.
- Qin N, Olcese R, Stefani E, Birnbaumer L (1998) Modulation of human neuronal α_{1E} -type calcium channel by $\alpha_2\delta$ -subunit. *Am J Physiol* 274:C1324–C1331.
- Schuster A, Lacinová L, Klugbauer N, Ito H, Birnbaumer L, Hofmann F (1996) The IV26 segment of the L-type calcium channel is critical for the action of dihydropyridines and phenylalkylamines. *EMBO J* 15:2365–2370.
- Shirokov R, Ferreira G, Yi J, Ríos E (1998) Inactivation of gating currents of L-type calcium channels. Specific role of the $\alpha_2\delta$ subunit. *J Gen Physiol* 111:807–823.
- Shistik E, Ivanina T, Puri T, Hosey M, Dascal N (1995) Ca^{2+} current enhancement by $\alpha_2\delta$ and β subunits in *Xenopus* oocytes: contribution of changes in channel gating and α_1 protein level. *J Physiol (Lond)* 489:55–62.
- Singer D, Biel M, Lotan I, Flockerzi V, Hofmann F, Dascal N (1991) The roles of the subunits in the function of the calcium channel. *Science* 253:1553–1557.
- Stefani A, Spadoni F, Bernardi G (1998) Gabapentin inhibits calcium currents in isolated rat brain neurons. *Neuropharmacology* 37:83–91.
- Strom TM, Nyakatura G, Apfelstedt-Sylla E, Hellebrand H, Lorenz B, Weber BH, Wutz K, Gutwilling N, Ruther K, Drescher B, Sauer C, Zrenner E, Meitinger T, Rosenthal A, Meindl A (1998) An L-type calcium-channel gene mutated in incomplete X-linked congenital stationary night blindness. *Nat Genet* 19:260–263.
- Taylor CP, Gee NS, Su T-Z, Kocsis JD, Welty DF, Brown JP, Dooley DJ, Boden P, Singh L (1998) A summary of mechanistic hypotheses of gabapentin pharmacology. *Epilepsy Res* 29:233–249.
- Welling A, Bosse E, Cavalié A, Bottlender G, Ludwig A, Nastainczyk W, Flockerzi V, Hofmann F (1993) Stable co-expression of calcium channel, α_1 , β and $\alpha_2\delta$ subunits in a somatic cell line. *J Physiol (Lond)* 471:749–765.
- Wiser O, Trus M, Tobi D, Halevi S, Giladi E, Atlas D (1996) The $\alpha_2\delta$ subunit of voltage sensitive Ca^{2+} channels is a single transmembrane extracellular protein which is involved in regulated secretion. *FEBS Lett* 379:15–20.